The Optimal Use of AI in Financial Regulation

Christopher Clayton* Antonio Coppola†

May 2026

Abstract

We study whether AI methods applied to large-scale portfolio holdings data can improve macroprudential financial regulation. We build a graph-based deep learning model tailored to security-level data on the holdings of financial intermediaries. The architecture incorporates economic priors and learns latent representations of both assets and investors from the network structure of portfolio positions. Applied to the universe of non-bank financial intermediaries, covering nearly $40 trillion in wealth, the model substantially outperforms existing approaches in out-of-sample forecasts of intermediary trading behavior, including in crisis episodes. The model has more than ten times the explanatory power for the cross-sectional variation in asset returns during stress events compared to traditional approaches, and it outperforms existing systemic risk metrics at the institution level. Its learned representations show that the holdings network encodes rich, economically interpretable information about fire-sale vulnerability. The architecture is fully inductive, producing informative estimates even when entire asset classes or investors are withheld from training. We embed our empirical approach into a macroprudential optimal policy framework to formalize why these objects matter for policy and welfare. We show that even in an equilibrium environment subject to the Lucas critique, the predictive information from the model improves welfare by sharpening the cross-sectional targeting of policy interventions, and we demonstrate a complementarity between prediction and structural knowledge.

Keywords: Artificial Intelligence, Graph Neural Networks, Holdings Data, Fire Sales, Macroprudential Policy, Asset Pricing, Embeddings, Stress Testing, Deep Learning, Transformers.

JEL Codes: C4, G1, G2.

*Yale School of Management and NBER; christopher.clayton@yale.edu.

†Stanford University Graduate School of Business and CEPR; acoppola@stanford.edu.

We thank Hui Chen, Maryam Farboodi, Paul Fontanier, Xavier Gabaix, Stefano Giglio, Guido Imbens, Hanno Lustig, Matteo Maggiori, Stefan Nagel, Pablo Ottonello, Markus Pelger, Ashesh Rambachan, Rob Richmond, Jann Spiess, and Stijn Van Nieuwerburgh for helpful comments. We also thank Oliver Wang and Zhongyu Yin for outstanding research assistance. This paper was previously circulated under the title *"Financial Regulation and AI: A Faustian Bargain?"*. Financial support from the Stanford GSB Business, Government, and Society (BGS) Initiative is gratefully acknowledged.

1 Introduction

A central task of macroprudential financial regulation is to identify where shocks will be amplified through the financial system and to intervene before the resulting price dislocations become socially costly. The information environment facing regulators has changed sharply: supervisory filings and security-level holdings records now provide granular data on portfolio positions across a large share of the financial system, while high-dimensional predictive methods have become dramatically more capable. This paper shows that deep learning models, when properly designed for the rich cross-section of holdings data now available, can substantially improve the measurement of financial fragility across multiple dimensions relevant for regulation: forecasting institutional trading, explaining crisis-period price dislocations, and measuring systemic selling pressure. We show that the structure of overlapping portfolios across financial intermediaries contains far more information about fire-sale vulnerabilities than is captured by existing approaches, and that this information can be recovered in an economically interpretable way. We complement our empirical analysis with a macroprudential optimal policy framework that provides one disciplined interpretation of when and why such predictive information can improve the targeting of policy interventions.

Learning effectively from data on institutional portfolios requires building models whose architecture appropriately reflects the structure of the problem, imposing a form of economic regularization. This motivates our focus on architecture design. Fire-sale dynamics, which are at the core of financial crises, are inherently a networked phenomenon: they propagate through the network of overlapping portfolios that connects investors and assets. For example, a fund forced to liquidate corporate bonds depresses prices for every other intermediary holding those same bonds, potentially triggering further rounds of forced selling. The cross-sectional pattern of who is likely to sell what in a crisis therefore depends on the full high-dimensional structure of portfolio overlaps across the financial system, not merely on the characteristics of individual investors or assets in isolation. Much of the modern deep learning toolkit, including sequence-based architectures that have been recently applied in asset pricing contexts, is designed for sequential or grid-structured inputs such as text and images. Yet in domains where the data has an important network structure, architectures tailored specifically to learn from it have led to major advances in performance (Jumper et al. 2021). We therefore design our deep learning approach to explicitly capture and make use of the full network structure of portfolios.

Specifically, we build a *graph transformer*, an attention-augmented graph neural network that learns latent representations of both investors and assets by iteratively propagating information along the holdings network. The architecture incorporates economic priors, for instance by using portfolio exposures as biases in its attention mechanism, so that positions of greater economic importance receive correspondingly greater weight in the information aggregation. We train the graph transformer on quarterly holdings data covering the positions of roughly 37,000 non-bank financial intermediaries in 85,000 assets, totaling nearly $40 trillion in wealth. Our empirical application focuses on non-bank financial intermediaries since they are an increasingly important source of fi-

nancial fragility, partly as a result of regulatory reform following the Great Financial Crisis. The model takes as input the current cross-section of portfolio holdings and a realized or scenario value of aggregate financial stress, and for each investor-asset pair it produces a forecast of the quantity change in each position. Hence the estimation target is the cross-sectional pattern of trading conditional on the aggregate state, not a forecast of the state itself—a distinction that, as we discuss, is directly relevant for regulatory applications. The primary value of holdings data in our approach therefore lies in predicting which investors will adjust which positions given the prevailing stress level, not in predicting whether a crisis will occur.

We demonstrate the performance of the model in three complementary dimensions that are relevant for financial regulation and macroprudential monitoring. First, under a strict walk-forward out-of-sample evaluation, in which the model is retrained each year and tested on strictly future data, the graph transformer substantially outperforms conventional balance-sheet measures, standard econometric methods, and alternative deep learning benchmarks in predicting financial intermediaries' trading behavior, including through crisis episodes. The model outperforms benchmarks on both the extensive margin (predicting which investor-asset positions are traded) and the intensive margin (how large trades are, conditional on trading). Importantly, we show the model generalizes inductively: even when entire asset classes (e.g., all corporate bonds) or entire sets of investors are withheld from training, it still produces informative forecasts for those unseen entities, confirming that the model learns underlying patterns and mechanisms of trading behavior that generalize beyond the specific sample seen during training.

Second, and of particular interest from an asset pricing perspective, the model's learned representations (embeddings) of assets and investors explain the cross-section of asset price dislocations during stress episodes, despite the model never having been trained on price or returns data. Traditional approaches to explaining crisis-period asset returns rely on collapsing the high-dimensional holdings data into a few low-dimensional summary statistics motivated by economic theory. We show that the graph transformer's embeddings deliver more than ten times the incremental explanatory power of these traditional summaries for the cross-section of bond returns in stress periods: 18 percentage points of incremental adjusted R-squared beyond standard asset characteristics, compared to roughly 1 percentage point from the best existing low-dimensional approaches. Intuitively, unlike traditional approaches, the model captures the entirety of the high-dimensional information in the data that is relevant for trading behavior and fire sale dynamics: for example, which positions are most crowded, which specific institutions are most exposed to funding instability, or where forced selling is likely to concentrate. We demonstrate empirically that an important dimension of the learned embeddings is economically interpretable: it captures the interaction of position crowdedness (concentration among flow-sensitive holders) and asset illiquidity. This single dimension accounts for roughly one quarter of the embeddings' explanatory power for crisis-period returns. Hence the model is recovering, from the data's relational structure, the economic forces that theory identifies as governing fire-sale amplification.

Third, as a systemic risk metric, the model's predicted selling intensity outperforms existing institution-level measures—including ΔCoVaR, fund outflows, trailing portfolio returns, and portfolio concentration—by a wide margin in the non-bank setting we study. We also construct prediction intervals around the model's forecasts using conformal methods, demonstrating that the uncertainty around these predictions can be quantified in a distribution-free manner across both calm and stress market regimes. Together, these results confirm that the holdings network contains predictive information about fire-sale dynamics that conventional low-dimensional summaries miss. When embedded in the policy framework, this recovered heterogeneity translates into better-targeted intervention and higher welfare.

Two additional properties of our deep learning architecture make it particularly well-suited to our setting. First, the model is permutation-invariant: predictions do not depend on the arbitrary ordering of investors or assets. This is a key distinction from sequence-based architectures such as the text transformers that underpin modern large language models, in which the order of tokens is essential to their contextual meaning. In our setting, permutation invariance respects a fundamental symmetry of the problem. Second, the graph transformer is inductive: all model parameters are fully shared across nodes, allowing the model to generalize to new investors or assets without retraining, as we verify empirically in practice. This is not merely a convenience but a practical necessity for regulatory deployment, where new entities continuously enter and exit the data. Parameter sharing also enforces a strong form of regularization, leading to strong generalization out of sample. Together, these properties lead to highly sample-efficient learning that distinguishes graph-based architectures from alternatives that treat the holdings matrix as an unstructured grid or sequence.

While the empirical objects that we study are of direct, independent interest for financial stability monitoring and macroprudential surveillance, we also develop a complementary theoretical framework that offers one disciplined interpretation of the policy and welfare value of these empirical objects. In particular, the theory lets us address the Lucas (1976) critique, a natural concern with deploying any reduced-form predictive model for policy: the model might forecast distress accurately, but the relationships it learns need not be invariant to the regulation itself. We characterize the regulator's optimal intervention and show that it decomposes into two inputs. The first is a set of structural elasticities: the causal impact of the regulator's policy instruments on equilibrium liquidation prices. The second is a set of cross-sectional targeting statistics: the forecasted pattern of forced selling across investors and assets that would prevail absent intervention (matching the empirical focus on trading behavior conditional on the aggregate state). The key implication is that a purely predictive model—i.e., one that is uninformative about policy counterfactuals—can improve welfare, provided it sharpens the regulator's forecast of these targeting statistics and the regulator has prior knowledge of the relevant structural elasticities.

We consider a standard fire-sale environment in which intermediaries, faced with binding collateral constraints, are forced to sell assets prior to maturity to second-best users. Intermediaries can choose which assets to sell, subject to their constraints, and assets may face different degrees of fire

sales. In this environment, we consider intervention by a regulator that can use a set of regulatory wedges in order to manage which assets are sold by intermediaries, for example, pushing intermediaries to sell assets with smaller fire sale impacts. The key information friction is that the regulator faces uncertainty about the underlying parameters that govern what assets intermediaries sell, and what the fire sale spillovers are. The regulator can choose to adopt a *model*, which is a process for drawing a signal of the true parameters, before intervening. The regulator's core question is where to intervene and by how much. Fire-sale externalities vary across markets: e.g., a dollar of forced selling in an illiquid corporate bond market may depress prices far more than the same selling in a liquid government bond market. So the regulator needs to know both which markets are under the most selling pressure and how its instruments translate into price changes in those markets. These are two different kinds of information.

We formalize this distinction by showing that under certain conditions on the information structure, the regulator's optimal intervention decomposes into two components,[1]

$$\underbrace{\tau^*}_{\text{Optimal Intervention}} = \underbrace{\Omega}_{\text{Causal Policy Impact}} \quad \underbrace{\hat{L}}_{\text{Predicted Selling}} .$$

The first term Ω corresponds to the structural elasticities capturing the regulator's causal policy impact: how the regulator's instruments change equilibrium selling, and how those changes move market-clearing prices. These depend on the depth of secondary markets, the binding constraints facing intermediaries, and the structure of demand from arbitrageurs. The cross-sectional targeting statistics $\hat{L}$ capture the predictive channel: the pattern of forced selling across investors and assets that would prevail absent intervention. The prediction of liquidations is important to the regulator because the social benefit of intervening on any margin is proportional to the amount of forced selling on that margin, which determines the amount of assets being revalued in the fire sale. A model that accurately forecasts where selling will concentrate therefore allows the regulator to target its intervention more precisely, even if the model says nothing about how intervention changes outcomes. This interpretation also clarifies why the natural empirical task is to predict the cross-sectional pattern of investor-level trading conditional on the aggregate state. This is the estimation target that we introduce in our empirical analysis.

We show that under certain conditions on the information structure, the structural loadings that translate portfolios and policy wedges into equilibrium outcomes are invariant to the regulator's model choice, even though intermediaries' ex ante portfolio decisions respond endogenously to the anticipated intervention, making the use of a predictive model robust to the Lucas critique. Intuitively, the robustness comes from the fact that in this framework, predictive models are not used for estimating policy counterfactuals, but simply to improve the cross-sectional targeting of the policy. The theory yields a complementarity result: predictive accuracy is most valuable precisely on

[1]The structure of this optimal wedge formula is familiar from the macroprudential policy literature (e.g., Farhi and Werning 2016), with our main insight being the implication for the use of predictive models in optimal policy.

the margins where the regulator's causal knowledge is strongest. It also shows that a weighted predictive R-squared, where the weights reflect the causal leverage of the policy, is a sufficient statistic for the welfare gains from a given predictive model, providing a direct bridge between out-of-sample forecast accuracy and the value of the model for regulation. We further study the feedback of model choice on ex ante portfolio decisions, characterize optimal ex ante macroprudential regulation, and extend the analysis to subsidy-based (bailout) interventions.

The broader contribution of the paper is to clarify the role of prediction in macro-policy problems. In policy environments with high-dimensional state spaces, reduced-form prediction can be valuable even when it is not a substitute for structural modeling: its role is to estimate the sufficient statistics that structural policy rules require for accurate targeting. Structural models remain necessary for disciplined counterfactuals and welfare analysis, while predictive models are valuable because they recover heterogeneity that is difficult to capture with structure alone. In this sense, the paper speaks both to macroprudential regulation and to a broader class of economic policy problems in which governments observe increasingly rich data but still need structurally disciplined rules for intervention.

Related Literature. Our analysis relates to several areas of the literature. First, we connect to the literature on applications of machine learning and deep learning to finance. Gu, Kelly and Xiu (2020, 2021), Kozak, Nagel and Santosh (2020), Nagel (2021), and Bryzgalova, DeMiguel, Li and Pelger (2023) apply machine learning techniques to the canonical empirical asset pricing problem of valuation in the cross-section of assets. Similarly, Chen, Pelger and Zhu (2024) introduce a deep learning architecture for modeling stock returns. Giglio, Kelly and Xiu (2022) review the intersection of empirical asset pricing and machine learning. Gabaix, Koijen, Richmond and Yogo (2024) use holdings data together with a variety of deep learning sequence models (e.g., Word2Vec and BERT) and recommender systems to estimate asset embeddings, and Gabaix, Koijen, Richmond and Yogo (2025) apply these to explain variation and volatility in credit spreads. Chen, Cheng, Liu and Tang (2023) study transfer learning problems to bridge structural and machine learning models in asset pricing. Dolphin, Smyth and Dong (2022) and Sarkar (2025) also construct asset embeddings, respectively from return data and textual sources. Bybee (2025) generates expectations from large language models and studies bubble dynamics. Cohen, Lu and Nguyen (2026) apply a recurrent network to predict the directions of mutual fund trades. Methodologically, our paper employs graph neural network architectures (Scarselli, Gori, Tsoi, Hagenbuchner and Monfardini 2008; Hamilton, Ying and Leskovec 2017; Xu, Hu, Leskovec and Jegelka 2018; Wu, Pan, Chen, Long, Zhang and Yu 2020) to learn representations from the relational structure of asset holdings data, and we show that explicitly modeling the graph structure of overlapping portfolios yields large predictive gains.[2]

Our applications of machine learning models for financial regulation relate to a longstanding debate, from Koopmans (1947) to Friedman (1953) and Lucas (1976), about whether predictive re-

[2]See also Elliott, Golub and Jackson (2014) and Acemoglu, Ozdaglar and Tahbaz-Salehi (2015) for theory highlighting the importance of the network structure of positions for financial stability.

lationships that are not themselves structural can inform policy. We show that sufficiently capable predictive models can have a role in the macro-regulatory toolbox, not as substitutes for structural models, but as complements that recover high-dimensional targeting statistics while structure disciplines counterfactuals.

Second, we connect to the literature on fire sales, and macroprudential regulation and ex-post interventions. Theoretical contributions include Bernanke and Gertler (1986), Williamson (1988), Kiyotaki and Moore (1997), Caballero and Krishnamurthy (2001), Lorenzoni (2008), Uhlig (2010), Bianchi (2011, 2016), Stein (2012), Farhi and Werning (2016), Chari and Kehoe (2016), Bianchi and Mendoza (2018), Dávila and Korinek (2017), and Clayton and Schaab (2022, 2025). On the empirical side, prior work has focused on particular variables to explain and predict the occurrence and magnitude of fire sales, such as leverage and maturity mismatches (Fisher 1933; Kindleberger and Aliber 1978; Brunnermeier and Oehmke 2013; Schularick and Taylor 2012; Adrian and Shin 2014; Adrian and Brunnermeier 2016; Acharya, Pedersen, Philippon and Richardson 2017; Krishnamurthy and Muir 2025) as well as investor composition (Brainard and Tobin 1968; Coval and Stafford 2007; Haddad, Moreira and Muir 2021; Coppola 2025; Fang, Hardy and Lewis 2025): the empirical contribution of this paper asks whether there is additional value from a more agnostic approach that does not impose an ex-ante focus on particular dimensions of the data.

Third, we relate to literature studying the deployment of machine learning and large-scale data for economic analysis and policy problems more broadly, including Einav and Levin (2014b,a), Kleinberg, Ludwig, Mullainathan and Obermeyer (2015), Athey (2017, 2018), Mullainathan and Spiess (2017), Kleinberg, Lakkaraju, Leskovec, Ludwig and Mullainathan (2018), Athey and Imbens (2019), Gillis and Spiess (2019), Farboodi and Veldkamp (2020), Athey and Wager (2021), and Fuster, Goldsmith-Pinkham, Ramadorai and Walther (2022). Relatedly, a recent literature in macroeconomics has highlighted how empirically identified causal effect estimates can be used to inform policy (Nakamura and Steinsson 2018, McKay and Wolf 2023). The question of how non-policy invariant relationships should be exploited by regulators also has earlier conceptual parallels, for instance by Barro and Gordon (1983) in the context of the Phillips curve. The model and information design aspect of our theoretical approach connects to work on stress testing (Shapiro and Skeie 2015; Faria-e Castro, Martinez and Philippon 2017; Goldstein and Leitner 2018; Leitner and Williams 2023; Orlov, Zryumov and Skrzypacz 2023; Parlatore and Philippon 2025).

2 Structure-Aware Deep Learning for Holdings Data

The defining feature of holdings data is rich relational structure: the data naturally represents a bipartite graph connecting investors and assets, with positions as edges. We build a *graph transformer*, an attention-augmented graph neural network (GNN) that learns latent representations of both investors and assets by iteratively propagating information along this holdings network (Scarselli et

al. 2008; Hamilton et al. 2017; Wu et al. 2020).[3] Three properties distinguish this architecture from alternatives. First, it learns directly from the graph structure of overlapping portfolios: through iterative *message passing*, each investor's embedding updates based on the embeddings of the assets it holds, and vice versa, so that information propagates through the network of portfolios. As we show in our analysis, this relational structure is the single largest source of the model's predictive advantage. Second, it is permutation invariant: predictions do not depend on the arbitrary ordering convention applied to investors or assets to represent portfolios, unlike sequence-based architectures in which token order is essential. In our setting, permutation invariance respects a fundamental symmetry of the problem. Third, because all parameters are shared across nodes, the architecture is inductive: it can produce embeddings and forecasts for new, unseen investors or assets without retraining, and we verify this inductive generalization capability empirically.

Estimation Objective. The goal of the empirical model is to learn how each investor in the financial system trades each asset in response to the prevailing state of the world. This cross-sectional prediction task is of direct empirical interest for financial stability monitoring, stress testing, and systemic risk measurement. As we discuss in Section 4, it also has a natural interpretation in terms of the targeting statistics relevant for optimal policy.

Formally, we let $\mathcal{G}_t$ denote the observed holdings data at time t: this is the full cross-section of who holds what, and how much, at the end of period t. We model $\mathcal{G}_t$ as a graph connecting investors to assets via their positions. We also let ζ_{t+1} be a scalar summary of the aggregate state at period $t+1$: this is a single number that summarizes the extent to which the period represents a stress regime or a calm regime. In our implementation, we use the Financial Stress Index (FSI) published by the St. Louis Fed as our aggregate state summary ζ_{t+1}, which is the first principal component of 18 time series indicators of financial market stress including the VIX and yield spreads.

We distinguish between market-value positions $w_{ia,t}$ and notional-quantity positions $q_{ia,t}$. The position $w_{ia,t}$ is the market value of investor i's holdings in asset a at time t, while $q_{ia,t}$ denotes the notional quantity (shares for equities, par value for bonds). For each investor-asset pair (i, a), we define the trade outcomes

$$y_{ia,t+1} = \log\left(\frac{q_{ia,t+1}}{q_{ia,t}}\right), \tag{1}$$

which capture the pure quantity change in investor i's position in asset a between the end of period t and the end of period $t+1$.[4] The central estimation target is the conditional trading response

[3] GNNs have achieved strong results in domains where relational structure is paramount, including protein structure prediction (Jumper et al. 2021), traffic forecasting (Derrow-Pinion et al. 2021), and drug discovery (Jiang et al. 2021). The architectural principle—that learning directly from relational structure improves prediction when the data is naturally graph-structured—transfers to the holdings setting, as our empirical results confirm.

[4] The log transformation places buys and sells on a symmetric scale, which facilitates the numerical learning: doubling a position and halving it yield targets of equal magnitude with opposite sign. In our implementation, we clip the values of $y_{ia,t+1}$ to the range $[-5, 5]$ to limit the influence of extreme outliers from very small initial positions. The target $y_{ia,t+1}$ is only defined for continuing positions with $q_{ia,t} > 0$:

function:

$$\hat{y}_{ia,t+1} = \hat{\mathbb{E}}\left[\underbrace{\log\left(\frac{q_{ia,t+1}}{q_{ia,t}}\right)}_{\text{Trade from } t \text{ to } t+1} \;\middle|\; \underbrace{\mathcal{G}_t}_{\text{Positions at } t}, \underbrace{\zeta_{t+1}}_{\text{Aggregate state}} \right] \quad \text{for all } (i,a). \tag{2}$$

That is, for each investor-asset pair (i, a), the model takes as inputs the current cross-section of portfolio positions $\mathcal{G}_t$ and a realized (or scenario) value of aggregate financial stress ζ_{t+1}, and produces a (conditional) forecast of the quantity change in each position over the subsequent period. These conditional expectations can be understood as reaction functions: given the configuration of the financial system at time t, they describe how each investor adjusts each position conditionally on a given level of aggregate financial stress.

Several features of the conditioning in equation (2) are worth emphasizing. First, the model does not forecast the aggregate state ζ_{t+1} itself. Rather, it takes ζ_{t+1} as given—either as a real-time observable that the regulator can measure when designing the intervention, or as a hypothetical stress scenario that the regulator can vary—and forecasts the cross-sectional pattern of trading responses conditional on that state. This conditioning structure is also natural from a regulatory perspective: a supervisor designing an intervention during a stress episode can observe the prevailing level of financial stress but needs to forecast how different institutions will respond to it. Second, the information set $\mathcal{G}_t$ consists entirely of time-t observables (current portfolio positions as well as the corresponding investor and asset characteristics) while the prediction target $y_{ia,t+1}$ is a forward-looking quantity that will be realized in the future.

We target the full cross-section of trading behavior $\{y_{ia,t+1}\}$ rather than crisis-period forced liquidations directly, for two reasons. First, forced liquidations are not directly observed: realized trades reflect the superposition of many motives, and isolating forced selling necessarily requires additional assumptions. Second, fire sale episodes are rare, so a model targeting crisis liquidations directly would face a severe small-sample problem; training on the broader task of predicting all trading behavior exploits far more data and learns general patterns of portfolio adjustment that are informative about the specific adjustments constituting fire sales. Our approach learns general-purpose representations of investors and assets from the full distribution of trading behavior, and we then verify empirically that these representations are informative about fire sale dynamics by showing that the learned embeddings explain the cross-section of asset price dislocations during market stress episodes (as shown in Section 3). When we consider empirical proxies for forced sales in Section 3.5, we show that the model performs especially well in predicting these.

new entries ($q_{ia,t} = 0$) are excluded from model training and evaluation. Thus, the baseline forecasting task focuses on adjustments of existing positions, while entry into entirely new positions is left outside the main target.

Core Architecture Specification. We now formally specify the GNN architecture used to estimate the conditional trading response functions in equation (2). We model holdings data using a graph data structure. The holdings graph $\mathcal{G}_t$ is bipartite: it has two distinct types of nodes, and edges only connect nodes of different types, with investors connecting to assets via position edges. Formally, at each time t, the holdings graph is $\mathcal{G}_t = (\mathcal{I}_t, \mathcal{A}_t, \mathcal{E}_t)$, where $\mathcal{I}_t = \{1, \ldots, I_t\}$ is the set of investors, $\mathcal{A}_t = \{1, \ldots, N_t\}$ is the set of assets, and $\mathcal{E}_t$ is the set of edges (i.e., positions). Whenever investor i holds asset a at time t, then $(i, a, w_{ia,t}, q_{ia,t}) \in \mathcal{E}_t$.[5] We write $\mathcal{V}_t = \mathcal{I}_t \cup \mathcal{A}_t$ as the set of all nodes, both assets and investors, and let $\mathcal{N}_t(v)$ be the neighborhood set for a given node v, which is the set of all nodes connected to v at time t. For assets, $\mathcal{N}_t(v)$ corresponds to the investors holding the asset, while for investors this corresponds to the set of assets in the investor's portfolio. Each node $v \in \mathcal{V}_t$ also has an associated set of characteristics $x_{v,t}$. The characteristics can be either numerical (e.g., the total amount outstanding of a given security) or categorical (e.g., the type of institutional investor).[6]

The model learns latent representations—vector embeddings—of each investor and asset at progressively richer levels of information aggregation. The initial asset and investor embeddings $h_{v,t}^{(0)}$ are obtained by mapping each node's observable characteristics $x_{v,t}$ into a d_h–dimensional vector via a learnable function ϕ:

$$h_{v,t}^{(0)} \;=\; \phi(x_{v,t})\,. \tag{3}$$

These initial embeddings are then refined through several successive layers of message passing, the core of the architecture, in which each node's representation updates based on the representations of its neighbors in the holdings network. Each message-passing layer integrates an attention mechanism that learns which positions should receive greater or lesser weight when aggregating information from neighboring nodes.

We perform L layers of message passing. At each layer ℓ, the prior-layer embeddings are first passed through a learned function $M^{(\ell)} : \mathbb{R}^{d_h} \to \mathbb{R}^{d_h}$ to construct *node messages*:

$$M_{v,t}^{\ell} = M^{(\ell)}(h_{v,t}^{(\ell-1)}). \tag{4}$$

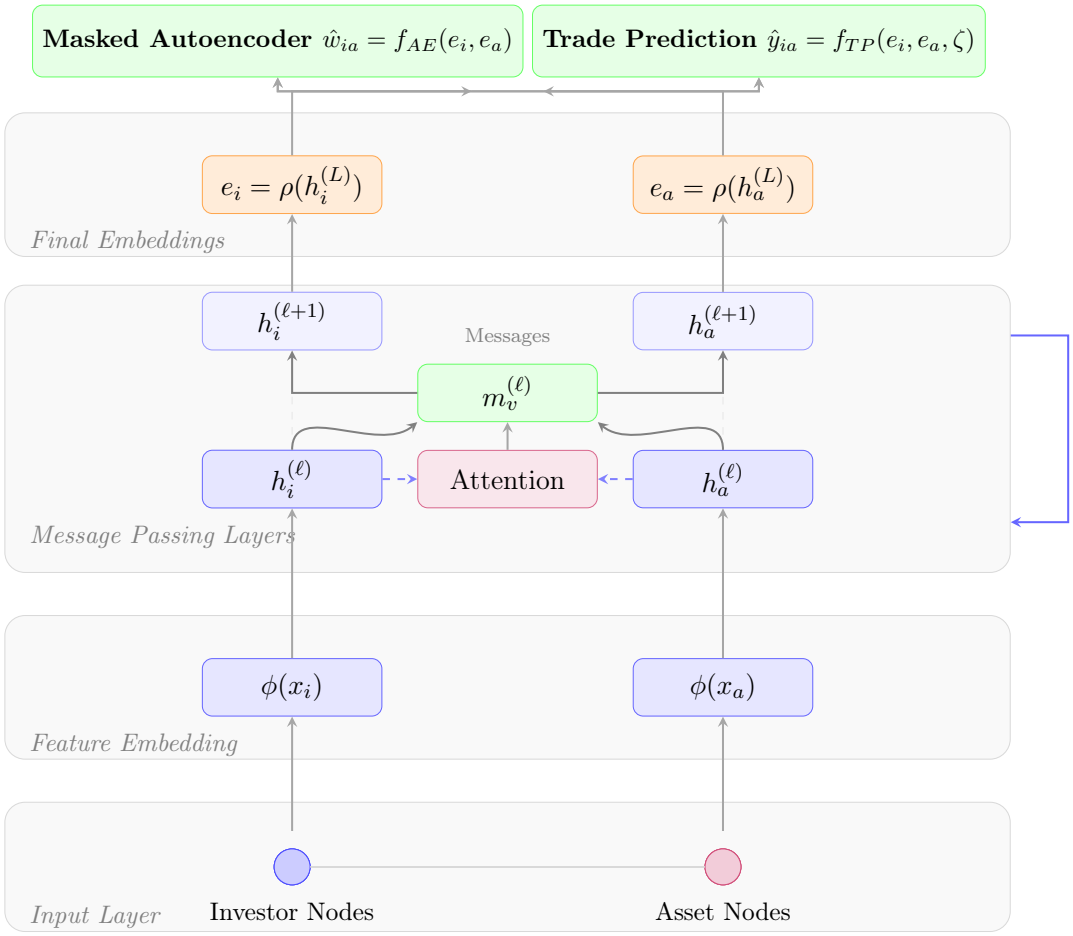
We incorporate the economic importance of each position (an economic prior) using a normalized edge exposure $\tilde{w}_{vu,t} \in (0, 1]$, which is constructed from the raw market-value position $w_{vu,t}$ by normalizing within each node's neighborhood:

$$\tilde{w}_{vu,t} \;=\; \frac{w_{vu,t}}{\sum_{k \in \mathcal{N}_t(v)} w_{vk,t}} \qquad \text{for } u \in \mathcal{N}_t(v). \tag{5}$$

[5] The positions can alternatively be written as $w_{ai,t} = w_{ia,t}$ and $q_{ai,t} = q_{ia,t}$. We allow for both notations so as to keep the rest of the formal architecture specification symmetric.

[6] Categorical features are embedded into a vector space of dimension d_c using functions that are learned jointly with the rest of the model's parameters, and then they are concatenated with numerical feature to form a single characteristics vector $x_{v,t}$.

Figure 1: **The graph transformer architecture**



Notes: We visualize the graph transformer architecture. Observable characteristics of each investor and asset node are mapped into initial embeddings via a learned function ϕ, then refined through L rounds of message passing in which nodes exchange information with their neighbors in the holdings network, with attention mechanisms determining the weight each position receives. A layer ρ produces final embeddings e_i and e_a, which feed into two heads: a masked autoencoder for pretraining on co-holding patterns and a trade prediction head for the supervised forecasting task. All learned functions (ϕ, $M^{(\ell)}$, $U^{(\ell)}$, ρ, and the prediction heads) are parameterized as feed-forward neural networks.

This ensures that a node's attention is concentrated on its economically important positions.

The architecture uses S_A independent attention heads with scaled dot-product queries and keys (Vaswani et al. 2017). For each head, learnable projection matrices produce query, key, and value representations from the node embeddings. The attention weights incorporate the normalized edge exposure $\tilde{w}_{vu,t}$ as an additive log-bias. The attention-weighted messages from each head are then averaged to produce the aggregated message $m_{v,t}^{(\ell)}$ for each node. Full details of the attention computation are provided in Appendix B.

The embeddings are then updated by combining each node's current embedding with its aggregated messages via a learned function $U^{(\ell)} : \mathbb{R}^{2d_h} \to \mathbb{R}^{d_h}$:

$$h_{v,t}^{(\ell)} = U^{(\ell)}(h_{v,t}^{(\ell-1)}, m_{v,t}^{(\ell)}). \tag{6}$$

After L rounds of message-passing, a readout layer $\rho : \mathbb{R}^{d_h} \to \mathbb{R}^{d_e}$ produces final asset and investor embeddings:

$$e_{v,t} = \rho(h_{v,t}^{(L)}). \tag{7}$$

When referring to node embeddings in subsequent sections, unless otherwise specified we refer to these final representations $e_{v,t}$.

Training Strategy. The model is trained in two sequential phases (Devlin et al. 2019; He et al. 2022). In the first phase (self-supervised pretraining), we train the GNN backbone using a masked autoencoder (MAE) objective: the model randomly masks a subset of edges in the graph and learns to reconstruct the masked position sizes. This forces the model to learn which positions tend to co-occur—discovering latent similarities among investors and assets from the pattern of who holds what—before it sees any information about trades. In the second phase (supervised training), we freeze the MAE head and fine-tune the GNN backbone using the supervised trade prediction head, which provides our estimates of the conditional response functions defined in equation (2).

Prediction Heads. The supervised prediction head takes the form of a hurdle model, motivated by the fact that approximately 40% of existing positions see no change in quantity in any given quarter. Without separating the two margins, the model would effectively average over the zero and nonzero trades, performing poorly at both predicting which positions are traded and predicting the size of trades that do occur. The hurdle model decomposes the prediction into two components: (i) an extensive margin prediction of whether a trade occurs at all, and (ii) an intensive margin prediction of the trade's magnitude, conditional on it occurring. The trade prediction head uses the concatenated investor and asset embeddings $(e_{i,t}, e_{a,t})$ together with the aggregate state ζ_{t+1} as inputs, branching into classification logits $\hat{c}_{ia,t+1}$ and a regression prediction $\hat{m}_{ia,t+1}$. The combined prediction is:

$$\hat{y}_{ia,t+1} = \sigma(\hat{c}_{ia,t+1}) \cdot \hat{m}_{ia,t+1}, \tag{8}$$

where $\sigma(\cdot)$ is the sigmoid function. The supervised objective combines binary cross-entropy for the extensive margin and mean squared error for the intensive margin. The MAE and supervised losses, along with the full specification of the training procedure, are detailed in Appendix B. We optimize all model parameters using the AdamW optimizer (Kingma 2014; Loshchilov and Hutter 2018).

The model architecture is summarized in Figure 1. We validate these architectural choices empirically in Section 3.2, where ablation experiments confirm that the graph structure is the primary source of predictive information.

Table 1: **Summary statistics**

	Mean	Std	P10	Median	P90	*N*
Panel A: Graph structure (per quarter)						
Investors	17,751	6,290	9,121	17,408	25,389	72
Assets	33,302	11,623	16,060	35,178	46,609	72
Holdings (edges)	2,310,818	1,172,503	900,260	2,043,472	4,091,039	72
Positions per investor	122.8	22.6	98.7	115.8	160.5	72
Holders per asset	65.6	13.2	55.7	58.5	88.2	72
Graph density (%)	0.406	0.125	0.307	0.352	0.615	72
Panel B: Holdings characteristics (pooled)						
Log holding value	12.60	3.58	9.44	13.11	16.01	166,378,929
Holding value ($M)	5.8	29.9	0.0	0.5	9.0	166,378,929
Trade target ($y_{ia,t}$)	0.005	0.899	-0.277	0.074	0.348	149,755,712
Panel C: Investor characteristics (pooled)						
Total AUM ($M)	790.5	4929.1	13.4	120.3	1259.0	1,270,517
Number of positions	130.26	323.75	5.00	49.00	282.00	1,278,103
Equity share	0.49	0.47	0.00	0.56	1.00	1,278,103
Bond share	0.33	0.45	0.00	0.00	1.00	1,278,103
Panel D: Asset characteristics (pooled)						
Total held value ($M)	418.9	2149.7	7.7	78.2	644.7	2,397,769
Number of holders	69.40	145.68	2.00	23.00	165.00	2,397,769
Coupon (%)	4.60	7.81	1.25	4.75	7.31	1,335,690
Years to maturity	9.10	9.93	1.37	5.83	24.30	778,007

Notes: Panel A reports summary statistics of the holdings data at the quarterly level, across 72 quarters from 2004Q1 to 2021Q4. Panels B–D report summary statistics pooled across all investor-asset-quarter observations. Holdings data are from Factset and Morningstar and cover non-bank financial intermediaries including mutual funds, ETFs, separate accounts, pensions, and insurance companies. Holding value is the dollar value of each position. Trade targets are the log position quantity change, $\log(q_{ia,t+1}/q_{ia,t})$. Investor and asset characteristics are the node features used as model inputs. "Total AUM" is total assets under management; "Total held value" is the aggregate dollar amount held by all investors in a given security.

3 Empirical Implementation and Results

We implement and evaluate the graph transformer on holdings data covering nearly $40 trillion in non-bank intermediary wealth. We assess the model along three dimensions relevant for financial regulation: forecasting institutional trading behavior, explaining the cross-section of asset price dislocations during stress episodes, and measuring systemic risk at the institution level. We also construct distribution-free prediction intervals around the model's forecasts.

3.1 Setting, Data, and Model Training

We implement our empirical approach in the setting of non-bank financial intermediation. Since the Great Financial Crisis, tighter bank regulation (e.g., leverage and proprietary-trading constraints) has reduced dealer balance-sheet intermediation and pushed a larger share of risk-taking and liquidity transformation into non-banks, such as money market funds, funds holding bonds and collateralized loan obligations, ETFs, insurers, and pensions. These institutions now intermediate a substantial fraction of tradable credit and duration risk and are subject to fire-sale amplification mechanisms such as runnable or flow-sensitive funding and mark-to-market constraints (Chen et al. 2010; Goldstein et al. 2017; Aramonte et al. 2023; Coppola 2025). Therefore they have become central to episodes where widespread price dislocations occur: for instance, acute liquidity needs by bond mutual funds played a key role in debt market disruptions in the first quarter of 2020 (Haddad, Moreira and Muir 2021; Ma, Xiao and Zeng 2022).

Table 2: **Model hyperparameters**

A. Architecture	
Hidden dimension (d_h)	256
Embedding dimension (d_e)	128
Message-passing layers (L)	3
Attention heads (S_A)	4
Categorical embedding dimension (d_c)	16
Dropout rate	0.1
B. Training	
MAE pretrain epochs	50
Supervised fine-tune epochs	500 (early stopping)
Learning rate	10^{-3}
Weight decay	10^{-2}
Edge masking rate (MAE)	0.35

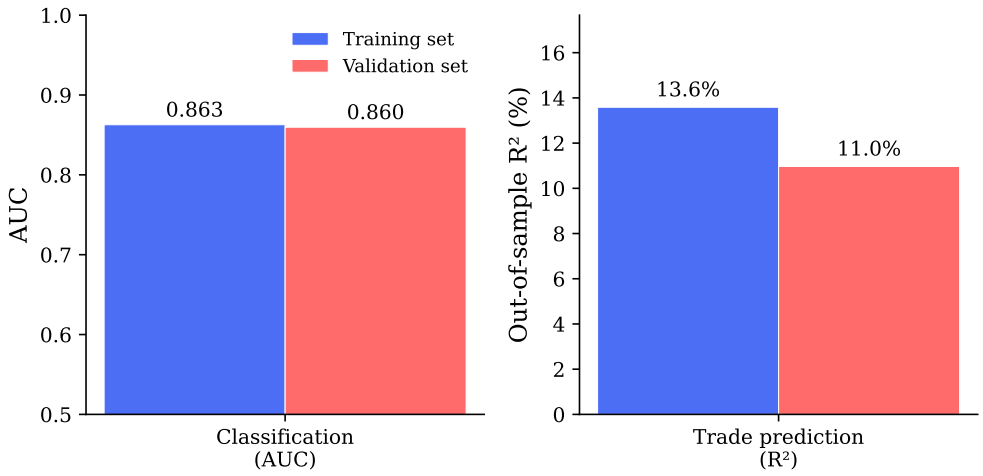
Notes: We list the hyperparameters used for our graph transformer architecture and in the two-phase training procedure.

We train our deep learning model on quarterly institutional holdings from Factset and Morningstar, starting in 2004Q1, which cover a broad range of non-bank intermediaries including mutual funds, ETFs, separate accounts, pensions, and insurance companies. The holdings data gives us

observations of the positions graph $\mathcal{G}_t$ for each quarter's cross-section, and we also use it to construct the trade outcomes $y_{ia,t+1}$. Table 1 reports summary statistics for the holdings data. Across all quarters, the data covers the positions of roughly 37,000 unique non-bank financial intermediaries in 85,000 unique assets.

We evaluate the model using two complementary out-of-sample strategies, and we report results under both throughout the paper. The first is a *static split*, in which quarters are randomly partitioned into training and validation sets; this approach maximizes the available training data and provides a pooled measure of predictive accuracy. The second is a *walk-forward* evaluation, in which the model is retrained from scratch each year on an expanding window of past data and tested strictly on the subsequent year's quarters, mimicking real-time regulatory deployment. The walk-forward evaluation spans six annual windows from 2015 to 2020, with the final window providing a particularly salient test during a crisis event: the model is trained only on pre-crisis data and then evaluated on the Covid-19 stress episode (2020q1).

Figure 2: **Performance metrics: static OOS split**



Notes: We plot the out-of-sample performance of the trade prediction hurdle model's two components under the static split: the classification AUC for predicting whether a trade occurs (left panel) and the regression R^2 on nonzero $y_{ia,t+1}$ targets (right panel). The blue bars show performance on the training set, while the red bars show out-of-sample performance on the validation set.

We construct the node feature vectors x_v using reference information from Factset, Morningstar, and the GCAP security master file. For assets, the feature vectors x_v include asset class, currency of denomination, amount outstanding, number of holders, average position size, standard deviation of position size, as well as bond sub-class and coupon for debt securities. For investors, they include institution type (such as open-end mutual funds, ETFs, separate accounts, etc.), manager style (including flags for active vs. passive portfolio management and strategy types), total AUM, number of positions, average position size, and standard deviation of position size.[7]

[7]In principle, our architecture also allows for the use of global features that vary over time but not across

Hyperparameters are chosen as in Table 2. We set the hidden dimension to $d_h = 256$ and the final embeddings dimensionality to $d_e = 128$. We use $L = 3$ layers of message-passing with $S_A = 4$ attention heads per layer. We do not increase L beyond this number to prevent the over-smoothing problem, whereby the node embeddings would converge to similar values: intuitively, over-smoothing occurs for higher numbers of message-passing iterations since each consecutive iteration increases the *receptive field* of each node, i.e. the set of nodes that the final-layer embeddings attend to, and for high L values the receptive fields of all nodes converge to the largest possible field, which is the set of all nodes in the graph. The backbone and hurdle head together have approximately 1.3 million parameters.[8]

3.2 Assessing the Model's Predictive Performance

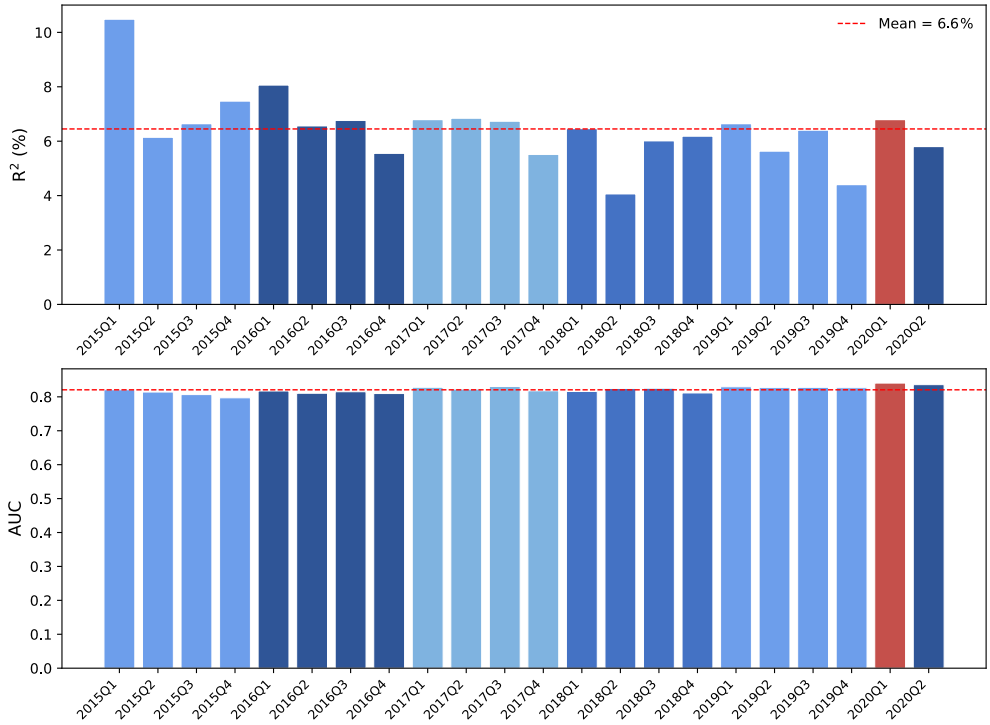
We evaluate the model under both out-of-sample strategies. Under the static split, the hurdle model achieves an out-of-sample classification AUC of 0.86 (the AUC measures how well the model distinguishes positions that will be traded from those that will not, with 1.0 indicating perfect separation and 0.5 indicating no discriminatory power) and a regression R^2 of 11.0% on nonzero trades, with minimal degradation from training to validation sets (Figure 2). Under the walk-forward evaluation, the model achieves an average R^2 of 6.6% and AUC of 0.823 across the six annual windows (Figure 3, Table 3), with stable performance throughout the evaluation period. The walk-forward R^2 is lower than the static-split R^2 due to two factors. First, the walk-forward windows train on fewer quarters (as few as 36 in the earliest window), reducing the model's effective training sample. Second, the random static split creates potential information leakage through the persistence of the holdings graph. The walk-forward design eliminates this channel entirely and therefore provides a more conservative measure of the model's predictive accuracy in a real-time regulatory deployment. In the 2020 window, the model achieves a walk-forward R^2 of 7.0%, and the per-quarter R^2 for 2020Q1—the peak of the Covid-19 market stress episode—is 6.8%. The classification AUC is nearly identical across both evaluation settings. The fully inductive design, sharing parameters across nodes and layers, ensures stable performance on unseen investors and assets, such that the model performs very similarly out-of-sample as it does on the training data.

Figure 4 shows a binned scatter plot of predicted vs. realized trades $y_{ia,t+1}$: the OLS slope through the bin means is 0.44, confirming that the model's predictions are informative for all levels of trading outcomes (both buying behavior and selling behavior) and that they are approximately well-calibrated. Figure 5 provides a portfolio sort of realized $y_{ia,t+1}$ by decile of the model's predicted

nodes during message-passing: these can be introduced as vectors which enter message-passing in the same way for all nodes in a given time period.

[8] We introduce dropout during training for additional regularization, with a dropout rate of 0.1. The AdamW optimizer uses a starting learning rate of 10^{-3} with weight decay of 10^{-2} and learning rate reduction on plateau. The self-supervised MAE pretraining phase runs for 50 epochs with a 35% edge masking rate; the supervised fine-tuning phase runs for up to 500 epochs with early stopping (patience of 5 epochs) based on the validation regression correlation. We train the model on four NVIDIA H100 GPUs.

Figure 3: **Walk-forward out-of-sample R^2 and AUC, by quarter**



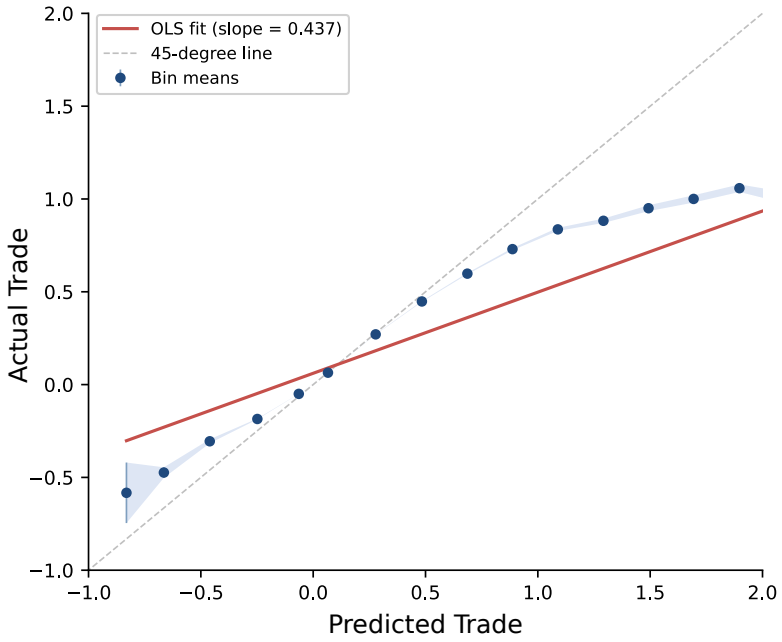
Notes: Per-quarter R^2 (top panel) and classification AUC (bottom panel) from the walk-forward trade prediction evaluation. Each bar represents one quarter that is strictly out of sample: the model used to generate each prediction was trained only on preceding quarters. Different shades of blue indicate different walk-forward windows. The red bar highlights 2020Q1, the onset of the Covid-19 crisis. Red dashed lines show means across periods.

Table 3: **Walk-forward temporal out-of-sample test, detailed statistics**

Test Year	Training Qs	AUC	Reg. Corr.	R^2 (%)	Comb. Corr.	Observations
2015	43	0.809	0.297	8.4	0.256	9,295,984
2016	47	0.813	0.277	6.7	0.223	10,405,466
2017	51	0.825	0.283	6.5	0.207	10,804,831
2018	55	0.819	0.263	5.7	0.214	11,735,336
2019	59	0.828	0.252	5.8	0.210	13,107,196
2020	63	0.839	0.289	7.0	0.232	13,415,123
Average	—	**0.823**	**0.276**	**6.6**	**0.223**	68,763,936

Notes: We show detailed results from the walk-forward out-of-sample test for the trade prediction task. The model is trained from scratch in each window. For each window, we show the number of training quarters. AUC measures the extensive margin classification of trade vs. no-trade. Regression correlation (Reg. Corr.) and R^2 are computed on non-zero target edges. Combined correlation (Comb. Corr.) uses combined predictions on the intensive and extensive margins ($\sigma(\hat{c}) \times \hat{m}$) from the full hurdle model.

Figure 4: **Binned scatterplot: predicted vs. actual trades** $y_{ia,t+1}$



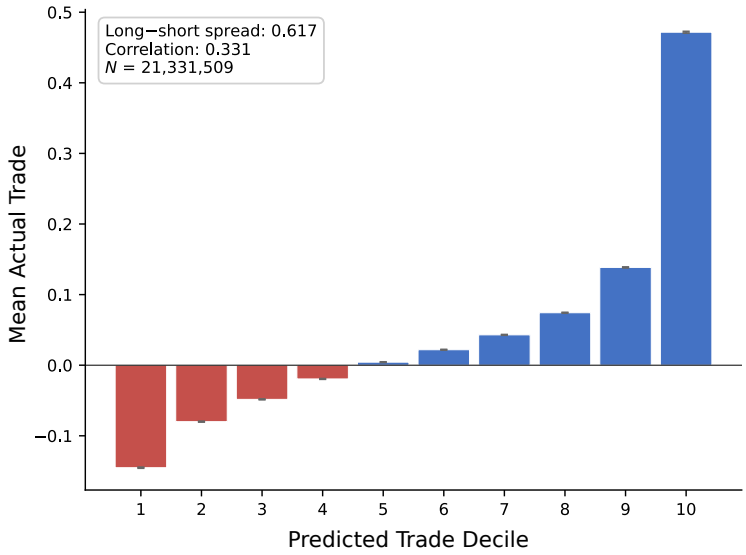
Notes: Equal-width binned scatter plot of out-of-sample predicted trades $\hat{y}_{ia,t+1}$ (horizontal axis) against realized trades $y_{ia,t+1}$ (vertical axis). Each dot is the mean of one bin; shaded band shows 95% confidence intervals. The red line is the OLS fit through the bin means.

$\hat{y}_{ia,t+1}$: the monotonic increase from the bottom decile to the top decile further confirms that the predictions are informative across the full range of trade outcomes.

Table 4 compares the graph transformer against a suite of benchmark models, all trained on identical trade prediction targets and evaluated out-of-sample on the same held-out quarters. The comparison is organized to isolate the sources of predictive power: from simple forecasting rules and linear methods that use only observable investor and asset characteristics, through flexible nonlinear methods, to deep learning architectures that progressively exploit the relational structure of the holdings data.

We first consider a range of traditional econometric and statistical models, which reveal the difficulty of forecasting trades from characteristics alone. A persistence forecast—which predicts that each investor will repeat last quarter's trade in each asset—produces a negative out-of-sample R^2: investors who bought last quarter are, if anything, less likely to buy again. Ridge regression on investor and asset characteristics achieves an R^2 of just 2.1%, and gradient-boosted trees, which can capture nonlinear interactions among the same features, reach only 1.7%. The lesson from these baselines is that observable characteristics of investors and assets, even combined with flexible nonlinear methods, explain little of the high-dimensional cross-sectional variation in trading behavior. The predictive signal lies predominantly in the structure of who holds what, and how those positions relate to one another across the network.

Figure 5: **Portfolio sort: realized trades by decile of predicted $\hat{y}_{ia,t+1}$**



Notes: We sort all out-of-sample investor-asset-quarter observations into deciles based on the model's predicted trades $\hat{y}_{ia,t+1}$, and we plot the mean realized trade $y_{ia,t+1}$ within each decile. The sample pools nonzero trade targets across all out-of-sample quarters. Error bars show 95% confidence intervals for the decile means. Realized outcomes are winsorized at the 1st and 99th percentiles to limit the influence of extreme trades from small initial positions. The long-short spread is the difference in mean realized $y_{ia,t+1}$ between the top and bottom deciles.

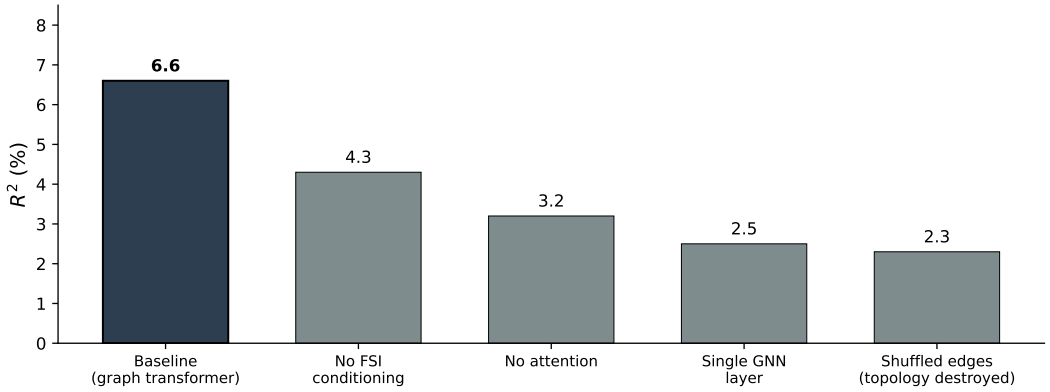
Next, we consider embeddings approaches which learn latent representations of assets and investors. The simplest such approach is a recommender system based on factorization of the holdings matrix, which achieves a walk-forward R^2 below 1%. We then introduce two deep learning models of our own that progressively exploit the holdings network's structure. Before going to the complete graph transformer, we also build a two-tower recommender system, a frontier recommender system approach, which is also our original contribution. The two-tower recommender learns separate latent embeddings for investors and assets and scores their interactions via an inner product, in the spirit of collaborative filtering, and it achieves an R^2 of 7.8%, roughly a fourfold improvement over the best traditional baseline. The two-tower model is inductive and generalizes to unseen entities, and it implicitly captures some relational structure through the shared embedding space, implementing some but not all of the features of the full graph transformer approach. The graph transformer goes further: it explicitly propagates information across the portfolio holdings network via attention-weighted message passing, capturing the full network structure. This yields an R^2 of 11%, a substantial improvement over all benchmarks. The walk-forward R^2 column confirms that this ranking is preserved in temporal out-of-sample evaluation, with the graph transformer again leading (with a more than 50% improvement in walk-forward out-of-sample R-squared compared to the next best model).

Table 4: **Trade prediction: comparison with alternative benchmarks**

Model	Ours	Graph	Inductive	AUC	R^2 (%)	WF R^2 (%)	Corr
A. Traditional models							
Persistence (lagged $y_{ia,t+1}$)				0.700	<0	<0	-0.054
Ridge regression				0.592	2.1	1.7	0.153
Gradient boosting				0.721	1.7	1.4	0.177
B. Latent-representation models							
Matrix-factorization recommender system				0.651	0.7	0.4	0.083
Two-tower recommender system	✓		✓	0.805	7.8	4.2	0.284
Graph transformer	✓	✓	✓	**0.860**	**11.0**	**6.6**	**0.331**

Notes: All models predict trades $y_{ia,t+1}$ on a held-out test set. "AUC" is the area under the ROC curve for predicting whether a trade occurs (nonzero target). "R^2" and "Corr" (Pearson correlation) are reported on the subset of edges with nonzero targets, measuring regression fit conditional on a trade occurring. "WF R^2" is the average R^2 from an expanding-window walk-forward test, where each model is retrained from scratch in each window and evaluated on future data only. "Ours" indicates models that are novel contributions of this paper. "Graph" indicates models that use the portfolio holdings network structure via message passing. "Inductive" indicates models that can generalize to unseen investors or assets without retraining.

Figure 6: **Architecture ablation study**



Notes: Walk-forward R^2 (%) for the baseline graph transformer and four ablation variants, each retrained from scratch in every expanding window. "No attention" replaces attention-based aggregation with symmetric mean pooling. "Single GNN layer" restricts message passing to one hop. "No FSI conditioning" removes the aggregate stress index ζ_{t+1} from the prediction head. "Shuffled edges" randomly permutes edge indices to destroy network topology while preserving node features and degree distributions.

Ablation Analysis. To investigate and isolate the sources of the empirical performance of the graph transformer model, we perform a series of ablation experiments, where we remove features of the model one at a time. Figure 6 reports walk-forward R^2 from these ablation experiments. The ablations show that the network information (the topology of the network) is indispensable: randomly shuffling edges, while preserving node features and degree distributions, reduces walk-forward R^2 from 6.6% to 2.3%, eliminating nearly two-thirds of the model's explanatory power and bringing the performance in line with models based only on characteristics. This confirms that the holdings network itself, not merely the flexible function approximation capacity of a neural network, is the primary driver of performance. Higher-order network structure is very important as well: restricting the model to a single layer of message passing, so that each node can only observe its immediate neighbors rather than aggregating information across higher degrees of network connections, reduces R^2 to 2.5%, a degradation nearly as severe as destroying the topology altogether. The attention mechanism, which allows the model to weight neighbors by economic importance rather than aggregating them symmetrically, contributes meaningfully, with its removal lowering R^2 to 3.2%. Finally, removing aggregate stress conditioning (ζ_{t+1}), which forces the model to infer the macroeconomic state implicitly from the high-dimensional portfolio data alone, reduces R^2 to 4.3%. That the model retains substantial predictive power even without this input suggests that the holdings network itself encodes a rich summary of the state that is relevant for forecasting aggregate conditions, though providing the state variable explicitly remains beneficial.

3.3 Explaining the Cross-Section of Returns in Stress Episodes

The graph transformer's embeddings, though never trained on price or returns data, are strongly informative about the cross-sectional variation in bond returns during stress episodes. Fire-sale events are rare, so we do not fit the model to them at training time. Instead, we ask whether the structure learned from the broader task of predicting trading behavior generalizes to explaining crisis-period price dislocations out of sample.

Traditional approaches to explaining crisis-period bond returns rely on collapsing the high-dimensional holdings data into a single low-dimensional summary statistic motivated by economic theory, and testing whether that statistic has predictive power for the cross-section of returns. For example, Coppola (2025) shows that the insurer share of a bond's investor base—i.e., the share of the bond held by insurance companies, a scalar summary of who holds the asset—predicts crisis-period returns because insurance companies are relatively stable holders that dampen fire-sale dynamics. We show that there is substantial additional information in the full high-dimensional holdings network, beyond what any single theoretically motivated summary captures.

Specifically, we focus on the cross-section of bond returns $r_{a,t}$ in the first quarter of 2020, during the Covid crisis—an episode featuring rapid and widespread disruptions in debt markets, partly driven by acute liquidity needs of investment funds and other non-bank intermediaries (Haddad et al. 2021; Ma et al. 2022). This event is fully outside of our training sample. For each bond, we use

the trained graph transformer applied to holdings data from 2019 to construct the prior-quarter embeddings $e_{a,t-1}$.[9] We estimate and compare cross-sectional specifications of the following form:

$$r_{a,t} = f(e_{a,t-1},\, X_{a,t-1}) + \varepsilon_{a,t} \tag{9}$$

$$r_{a,t} = f(\phi_{a,t-1},\, X_{a,t-1}) + \varepsilon_{a,t}, \tag{10}$$

where $X_{a,t-1}$ is a bond characteristics vector including bond rating and residual maturity and $\phi_{a,t-1}$ is the bond's insurer share. The first specification uses standard bond characteristics plus the graph transformer's learned embeddings. The second replaces the embeddings with the insurer share in the bond's investor base ($\phi_{a,t-1}$), a representative example of the traditional approach of using a single theory-motivated summary of the holdings data. This way, we can compare the relative explanatory power of these two approaches, which both use portfolio positioning to explain the cross-section of asset fire sales but in different methodological ways.

Table 5: **Explaining bond price dislocations**

	Embeddings Only	Embeddings and Characteristics	Traditional Approach
Cross-validated adjusted R^2			
Total	.08	.42	.24
Incremental to characteristics	—	.18	.01
Bond characteristics ($X_{a,t-1}$)		✓	✓
GNN embeddings ($e_{a,t-1}$)	✓	✓	
Insurer share ($\phi_{a,t-1}$)			✓
Observations (N)	4,771	4,771	4,771

Notes: Out-of-fold adjusted R-squared from gradient boosting models for the cross-section of bond returns in 2020Q1. "Embeddings" uses the graph transformer's prior-quarter asset embeddings $e_{a,t-1}$. "Traditional" uses the insurer share of each bond's investor base as a single theory-motivated summary of the holdings data, following Coppola (2025). Bond characteristics include rating and residual maturity. The incremental R-squared is the difference in adjusted R-squared between each specification and the characteristics-only baseline.

Given the high-dimensional nature of the embeddings $e_{a,t-1}$, we estimate a non-linear, nonparametric model: specifically, we estimate these specifications using gradient boosting with five-fold cross-validation. Table 5 reports the results. We report the out-of-sample adjusted R-squared both from a model which includes only the embeddings (column 1), a model which includes both the embeddings and bond characteristics (column 2), and a model which includes the insurer share and bond characteristics. For the latter two, we also report the incremental adjusted R-squared, which is the difference in the adjusted R-squared between the full model (including both $X_{a,t-1}$

[9] We use the sample of bonds that are reportable to TRACE, the transactions database maintained by FINRA. We apply to TRACE the data cleaning steps in Dick-Nielsen (2014), which are common in the literature. TRACE lets us observe the prices at which bonds transact. Quarterly bond returns account for price changes, coupons, and accrued interest, and they are constructed as in Coppola (2025).

and either $e_{a,t-1}$ or $\phi_{a,t-1}$) and a model including only characteristics. The incremental adjusted R-squared coming from the embeddings in the full model is 18%, and it is in fact higher than the value from the model which includes only the embeddings (as the full model, by virtue of being non-linear, also allows for interactions between the embeddings and the characteristics). The traditional approach—adding insurer share to the same characteristics—yields an adjusted R-squared to 24%, an incremental contribution of just 1 percentage point from the insurer share relative to characteristics.

The graph transformer's embeddings thus deliver more than ten times the incremental explanatory power of the traditional low-dimensional summary. This gap reflects the fundamental difference between the two approaches: the insurer share collapses the entire holdings network into a single scalar per asset, while the graph transformer's embeddings encode the full high-dimensional structure of who holds each bond, how those holders are connected through overlapping portfolios, and what the resulting patterns imply for the concentration of selling pressure during stress.[10] In Section 3.6, we show that the embeddings' explanatory power for the cross-section of crisis-time bond returns is concentrated in a specific, economically interpretable dimension capturing positioning: the interaction of position crowdedness and asset illiquidity that governs fire-sale externalities.

3.4 A Comparison With Systemic Risk Measures

Next, we consider the perspective of a regulator who is interested in monitoring systemic risk using institution-level metrics. We ask how our deep learning based approach compares to existing measures of systemic risk in identifying institutions that contribute most to selling pressure during stress periods in the non-bank setting that we consider. To evaluate different systemic risk measures, for each investor i and quarter t, we define the realized investor selling intensity as

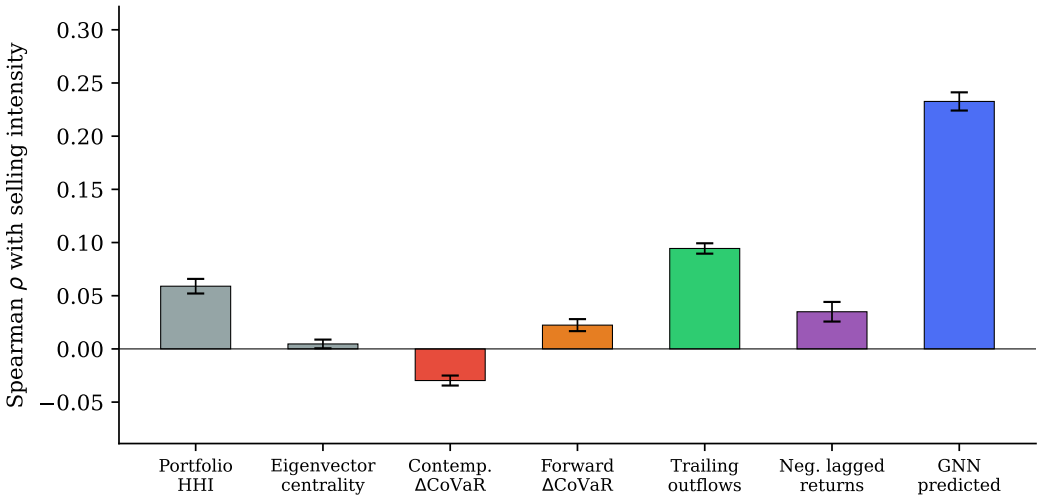
$$S_{i,t} \;=\; \frac{1}{\text{AUM}_{i,t-1}} \sum_{a} w_{ia,t-1} \max\left(-\frac{q_{ia,t} - q_{ia,t-1}}{q_{ia,t-1}},\, 0\right), \tag{11}$$

which measures the fraction of assets under management that an investor sells in a given quarter. Scaling by $1/\text{AUM}_{i,t-1}$ removes the mechanical size channel (larger investors sell more in absolute terms) and isolates the genuinely informative variation in selling behavior. For each out-of-sample quarter, we compute the Spearman rank correlation between each candidate systemic risk measure and the realized selling intensity across all investors.

We compare seven measures of systemic risk in our non-bank setting. The first is the ΔCoVaR measure introduced by Adrian and Brunnermeier (2016) in a banking context, which quantifies the increase in the financial system's tail risk conditional on a given institution being in distress. We

[10] Naturally, this does not imply that one approach dominates the other. Rather, they offer complementary methodological perspectives: the traditional approach has many advantages such as its transparency, straightforward insight into the economic mechanism, and the relative ease in applying reduced-form causal inference techniques.

Figure 7: **Systemic risk identification: comparing methods**



Notes: We plot the average Spearman rank correlation between each systemic importance measure and realized dollar-weighted selling pressure across investors, computed out of sample. Error bars show standard errors across quarters. Contemporaneous ΔCoVaR follows the Adrian and Brunnermeier (2016) methodology, estimated from monthly fund NAV returns. Forward ΔCoVaR is a linear prediction from lagged observable fund characteristics. Trailing outflows uses the negative of the percentage fund flow lagged one year. Negative lagged returns uses the negative of the previous quarter's compound gross return. GNN predicted selling uses the model's out-of-sample trade predictions.

estimate ΔCoVaR using monthly fund NAV returns, with a median of 119 months of data per fund over the 2003–2018 period, defining the system return as the AUM-weighted average monthly return across all funds, analogous to the value-weighted financial sector index used by Adrian and Brunnermeier (2016). For each fund, we estimate the 5th-percentile quantile regression of the system return on the individual fund return.[11] The second metric is a forward measure of ΔCoVaR, obtained by regressing the contemporaneous ΔCoVaR_i on lagged fund characteristics using OLS estimated on training data only, and applying the fitted model out of sample.

The third measure is portfolio concentration, as measured by the HHI of holdings. The fourth is eigenvector centrality of the portfolio overlap network, a simple theoretically motivated summary statistic for network structure. The fifth is trailing fund outflows, motivated by the flow-driven fire sale channel of Coval and Stafford (2007): funds experiencing outflows must liquidate holdings, so we use the lagged percentage fund outflow as a predictor of selling intensity. The sixth is negative lagged fund returns, motivated by the flow-performance relationship that is well-documented in

[11] Let $R_{i,t}$ denote fund i's monthly gross return and $R_{\text{sys},t} = \sum_j w_j R_{j,t} / \sum_j w_j$ the AUM-weighted system return, where w_j is fund j's average assets under management. We estimate $Q_{0.05}(R_{\text{sys},t} \mid R_{i,t}) = \alpha_i + \beta_i R_{i,t}$ and compute $\Delta\text{CoVaR}_i = \hat{\beta}_i(\text{VaR}_{0.05}(R_i) - \text{median}(R_i))$, where $\text{VaR}_{0.05}(R_i)$ is the 5th percentile of fund i's monthly return distribution. Funds with fewer than 36 monthly observations are excluded. The resulting ΔCoVaR measures capture fund-level tail risk contributions estimated from approximately 20,800 funds with sufficient data.

the fund market (Chevalier and Ellison 1997): poor past returns trigger outflows, which in turn force selling. The seventh is the predicted selling intensity from our GNN model, $\hat{S}_i$, where $\hat{S}_{i,t} = \text{AUM}_{i,t-1}^{-1} \sum_a w_{ia,t-1} \max(-\hat{y}_{ia,t}, 0)$ uses the model's out-of-sample trade predictions.

Table 6: **Systemic risk identification: comparing methods**

	Spearman ρ with selling intensity		
Method	All quarters	Stress	Calm
Portfolio HHI	0.059	0.045	0.060
	(0.007)	(0.007)	(0.007)
Eigenvector centrality	0.005	0.003	0.005
	(0.004)	(0.003)	(0.005)
Contemporaneous ΔCoVaR	-0.030	-0.018	-0.031
	(0.005)	(0.010)	(0.005)
Forward ΔCoVaR	0.022	0.038	0.021
	(0.006)	(0.001)	(0.006)
Trailing fund outflows	0.094	0.083	0.096
	(0.005)	(0.011)	(0.005)
Neg. lagged fund returns	0.035	0.006	0.038
	(0.009)	(0.000)	(0.010)
GNN predicted selling intensity	**0.233**	**0.184**	**0.237**
	(0.009)	(0.012)	(0.009)

Notes: Each cell reports the average Spearman rank correlation between the given measure and realized selling intensity $S_{i,t}$, with standard errors across quarters in parentheses. GNN predictions are out of sample. Stress quarters are defined by the St. Louis Fed Financial Stress Index (FSI) being above 1.5.

Figure 7 reports the results for the Spearman rank correlation (across investors) between each systemic risk measure and realized selling intensity. Table 6 also shows the same metrics separately for stress quarters (defined as quarters in which the financial stress index exceeds a threshold, FSI $>$ 1.5) and non-stress quarters. The GNN achieves the highest rank correlation with selling intensity by a wide margin ($\rho = 0.23$). The next strongest measure is trailing fund outflows ($\rho = 0.09$), consistent with the flow-driven fire sale channel, although the GNN outperforms it by a factor of more than two. All other measures achieve significantly smaller correlations: negative lagged returns ($\rho = 0.04$), forward ΔCoVaR from fund characteristics ($\rho = 0.02$), portfolio HHI ($\rho = 0.06$), eigenvector centrality ($\rho = 0.01$), and contemporaneous ΔCoVaR ($\rho = -0.03$). The results are stable across stress and calm quarters.

The non-bank setting we study differs from the banking sector in a way that helps explain these results and that highlights the value of holdings-based approaches. For non-bank intermediaries such as mutual funds, the cross-sectional variation in systemic risk contribution is encoded primarily in the structure of who holds what: which funds hold concentrated positions in illiquid assets, which investor bases are dominated by flow-sensitive holders, where portfolio overlaps create channels for

contagion, and so on. This is precisely the information that the graph transformer extracts from the holdings network. Return-based systemic risk measures such as ΔCoVaR (Adrian and Brunnermeier 2016), MES (Acharya et al. 2017), and SRISK (Brownlees and Engle 2017) were designed for the banking setting, in which leverage, maturity mismatch, and balance sheet interconnections generate informative cross-sectional variation in return co-movements (Benoit et al. 2017). In that setting, larger and more leveraged banks have more volatile returns and stronger co-movement with the financial system, so return-based tail risk measures correlate with systemic importance. For mutual funds, however, these leverage-driven channels are largely absent. For example, a $100 billion equity index fund and a $100 million equity index fund holding the same stocks have essentially the same return beta with the financial system, despite contributing very differently to aggregate selling pressure. The holdings network captures exactly this variation, whereas measures relying solely on return time-series data face an inherent limitation in this sector.

Table 7: **Trade prediction: heterogeneity by investor type and asset class**

	N	AUC	Reg Corr	Reg R^2 (%)	WF R^2 (%)	Share (%)
Panel A: By investor type						
Open-end mutual funds	26.2M	0.837	0.326	10.6	6.8	72.9
ETFs	4.8M	0.902	0.359	12.6	7.1	13.3
Non-fund institutions	4.1M	0.847	0.308	9.5	2.4	11.3
Other funds	899K	0.840	0.302	8.9	5.9	2.5
Active funds only	31.2M	0.839	0.323	10.4	6.1	86.7
Panel B: By asset class						
Common equity	24.5M	0.812	0.334	11.1	6.6	68.2
Corporate bonds	7.0M	0.831	0.311	9.6	6.2	19.5
Sovereign bonds	1.9M	0.814	0.327	10.6	7.6	5.4
Fund shares	1.4M	0.823	0.359	12.9	8.6	3.8
Other fixed income	678K	0.765	0.302	9.0	6.7	1.9
All	**35.9M**	**0.860**	**0.331**	**11.0**	**6.6**	100.0

Notes: Out-of-sample trade prediction performance decomposed by investor type (panel A) and asset class (panel B) using the graph transformer model. AUC measures classification of trading vs non-trading edges. Regression correlation and regression R^2 are computed on the nonzero-target subset. Performance is evaluated on held-out validation and test quarters. WF R^2 reports the pooled walk-forward out-of-sample R^2 from expanding-window retraining.

3.5 Heterogeneity and Inductive Generalization Performance

Next, we investigate heterogeneity in the predictive performance of the GNN, and we also conduct "cold start" tests where we explicitly assess the inductive generalization abilities of the model. A natural question is whether the predictive ability of the model comes primarily from relatively more mechanical aspects of the data, such as by correctly assessing the trades of passive index-tracking

investors. Table 7 addresses this directly: the "active funds only" row evaluates the model only on trades by funds that are classified as active (i.e., that do not passively track an index), and it shows an AUC of 0.839 and regression R^2 of 10.4%. This is quantitatively very similar to the full-sample results. The model's predictive ability is thus not driven by mechanical passive rebalancing. Table 7 also further decomposes the model's out-of-sample trade prediction performance by investor type and asset class, reporting both the classification AUC and the regression R^2 on nonzero $y_{ia,t+1}$ targets. Panel A shows results separately for different types of institutions: open-end mutual funds, ETFs, other funds, and non-fund institutions. Panel B shows the results by asset class. The model performs well across investor types and asset classes, including those (like open-end funds and corporate bonds) that have been at the center of fire sale dynamics in recent episodes of market stress (Haddad, Moreira and Muir 2021; Coppola 2025).[12]

We conduct additional tests to validate the model's inductive generalization, i.e. its ability to make predictions for entities never seen during training. For each experiment, we remove an entire category of investors or assets from all training graphs and retrain the graph transformer model from scratch, then evaluate the trained model on the complete (unmodified) graphs. Table 8 reports the results, including both regression R^2 on nonzero $y_{ia,t+1}$ targets and classification AUC for the binary trade prediction. In all experiments, the model's accuracy on seen edges is not strongly affected by the holdout, indicating that removing entity types does not meaningfully degrade performance on the remaining entities. For the random holdout tests, the gap between held-out and seen R^2 is small (e.g., 9.5% vs. 9.7% for the cold start test where we randomly exclude 20% of assets during training, and 7.6% vs. 9.2% for the test which excludes a random 20% of investors), confirming that the model generalizes to arbitrary unseen entities with little degradation. Even in the most challenging cold start test where we drop an entire asset class (corporate bonds), the GNN continues to do well on the held-out set: in this test, despite not having been trained on any corporate bond observations, the model still generalizes successfully to the unseen asset class and achieves an R^2 of 4.2%, having learned generalizable patterns of portfolio behavior from other markets.

3.6 Economic Content of the Learned Embeddings

The preceding sections show that the graph transformer's embeddings have strong predictive and explanatory power. We now ask what economic structure they actually encode. A typical concern with high-dimensional predictive models is that they are black boxes: we show that in this case, we can instead unpack what the model learns in ways that are economically interpretable.

[12]The theory of fire-sale externalities that motivates our framework implies that the welfare-relevant trades are forced liquidations: i.e., sales driven by funding constraints rather than discretionary portfolio rebalancing. A natural question is whether the model's predictive ability extends specifically to these economically important trades. Following Coval and Stafford (2007), we define a trade as "plausibly forced" if it occurs at an open-end mutual fund experiencing concurrent negative fund flows: such funds must sell assets to meet redemptions, regardless of their assessment of asset fundamentals. We use Morningstar quarterly fund flow data to identify OEFs with negative percentage flows in crisis quarters. The graph transformer achieves an R^2 of 15.3% on forced trades, significantly higher than the baseline performance for voluntary trades.

Table 8: **Cold-start inductive generalization test**

Held-Out Group	% Edges	Reg. Corr.		R^2 (%)		AUC	
	Held Out	Held-Out	Seen	Held-out	Seen	Held-Out	Seen
Corporate bonds	19.5	0.231	0.329	4.2	10.7	0.761	0.819
Random 20% investors	21.1	0.307	0.321	7.6	9.2	0.824	0.847
Random 20% assets	20.1	0.312	0.317	9.5	9.7	0.846	0.847

Notes: We show inductive generalization ("cold start") test using the graph transformer model. For each row, the model is trained from scratch with the indicated entity group entirely removed from all training graphs, then evaluated on the complete (unmodified) graphs. "Held-out" edges are those touching at least one held-out entity; "Seen" edges connect only entities present during training. Reg. Corr. and R^2 are computed on nonzero (traded) edges only. AUC measures trade/no-trade classification accuracy. The random investor test holds out 20% of individual investors (consistent across quarters); the random asset test holds out 20% of individual securities.

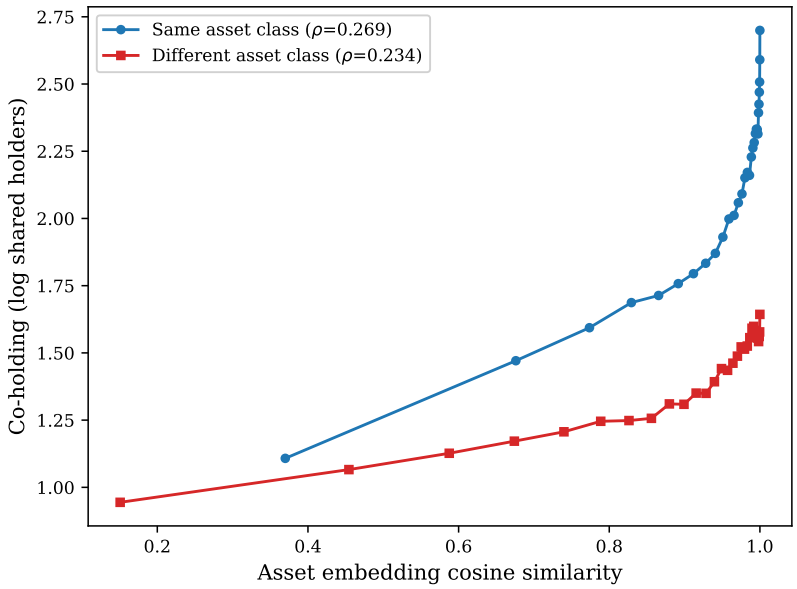
Dominant dimension: fire-sale vulnerability. We show that an economically significant dimension of the embeddings is their encoding of fire-sale vulnerability, captured by the interaction of position crowdedness and asset illiquidity. The fire-sale externality in Section 4 is proportional to the product of selling pressure (which is larger when positions are concentrated among flow-sensitive holders) and price impact (which is larger for illiquid assets). We construct a fire-sale vulnerability (FSV) index for each asset as the product of the fraction of holdings attributable to flow-sensitive investors (open-end mutual funds and ETFs) and a measure of asset illiquidity (inverse average daily volume). This FSV measure is not used in training the graph transformer; it is used only ex post to interpret the economic content of the learned embeddings. We then project the 128-dimensional asset embeddings onto the direction that best predicts the FSV score using ridge regression. This yields a scalar "FSV embedding projection" for each asset.

The embeddings predict the FSV score with a cross-validated R^2 of 11.5%, confirming that the GNN has learned to encode fire-sale vulnerability structure. More importantly, this FSV direction is disproportionately responsible for the embeddings' explanatory power for crisis-period bond returns. In the cross-sectional pricing specification of Section 3.3, removing the FSV direction from the embedding vector reduces the incremental R^2 from the embeddings by roughly one quarter. A placebo test using random embedding directions yields near-zero R^2, confirming that the FSV direction captures genuinely meaningful economic structure rather than statistical noise. Figure A.II (in the Appendix) visualizes the asset embedding space, using a two-dimensional t-SNE projection of the embedding vectors, colored by FSV quintile: high-vulnerability assets (Q5) cluster in distinct regions, consistent with the GNN learning how to position fire-sale-vulnerable assets in a recognizable pattern.

Supporting analyses. Two additional analyses corroborate that the embeddings capture economically meaningful structure beyond the FSV dimension. First, roughly half of the embedding

variation reflects novel structure not captured by observable characteristics: when we jointly regress each embedding dimension on all observable characteristics—including numeric features and one-hot encoded categorical features—the variance-weighted R^2 is 0.54 for investor embeddings and 0.50 for asset embeddings (Table A.I). The remaining variation is learned from the holdings network itself.

Figure 8: **Asset embedding similarity predicts co-holding**



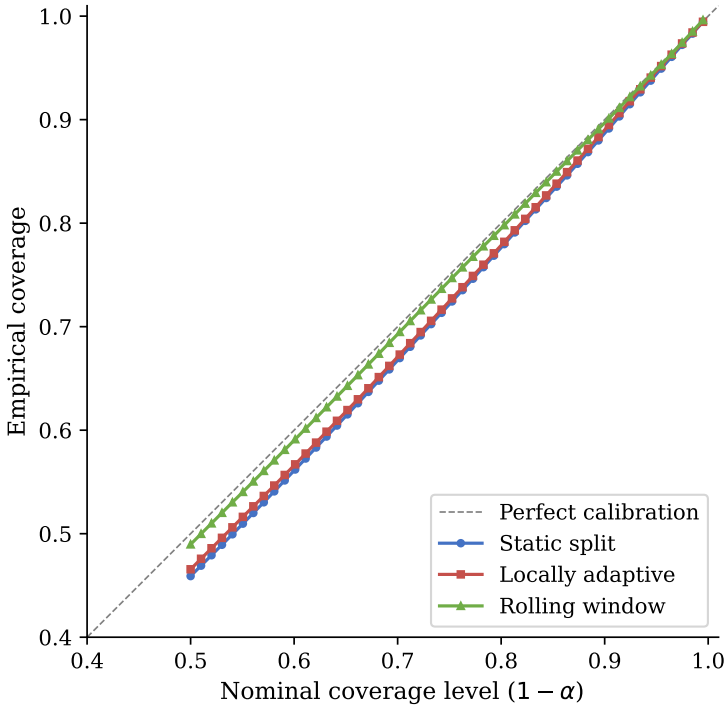
Notes: Binned scatter plot (30 equal-frequency bins) of pairwise co-holding (log number of shared investors) against pairwise asset embedding cosine similarity, for a sample of 3,000 assets restricted to pairs with at least one shared holder. Blue circles show same-class asset pairs; red squares show different-class pairs.

Second, we show that the embeddings capture co-holding structure, the patterns of common ownership that drive fire-sale contagion. For a sample of 3,000 assets, the pairwise cosine similarity of asset embeddings is positively and significantly correlated with pairwise co-holding ($r = 0.27$, $p < 0.001$; Figure 8). This correlation holds within same-class asset pairs, confirming that embedding similarity captures co-holding structure beyond what asset-class labels provide. Assets held by the same investors are likely to be traded together during portfolio rebalancing, and the graph transformer's learned embeddings internalize this common-ownership signal through message passing over the holdings network.

3.7 Conformal Prediction Intervals

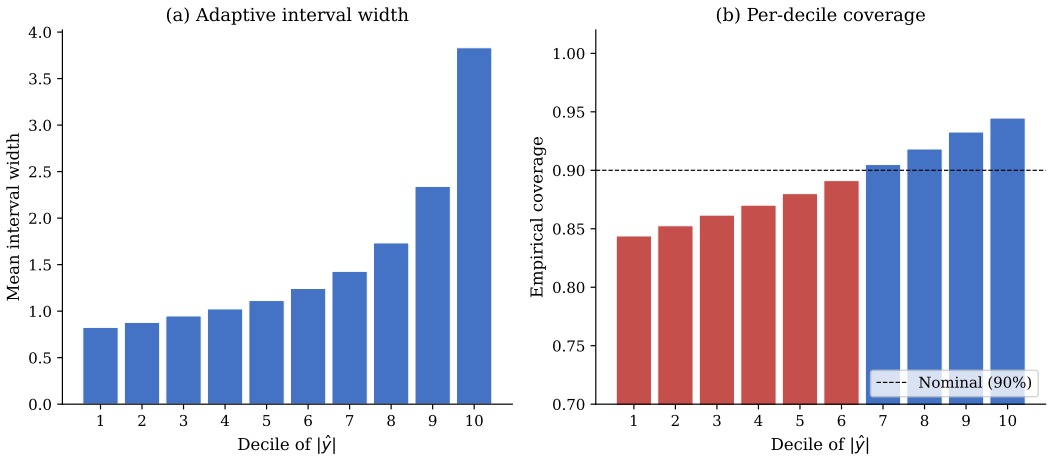
Point predictions are especially useful for regulatory decision-making if they are supplemented with measures of uncertainty. To provide useful ranges, we accompany each point forecast with a prediction interval using split conformal prediction (Vovk et al., 2005; Lei et al., 2018). Standard split conformal prediction guarantees finite-sample marginal coverage under exchangeability of calibration and test observations (Angelopoulos and Bates, 2023). Because our panel data are subject

Figure 9: **Conformal prediction: coverage calibration**



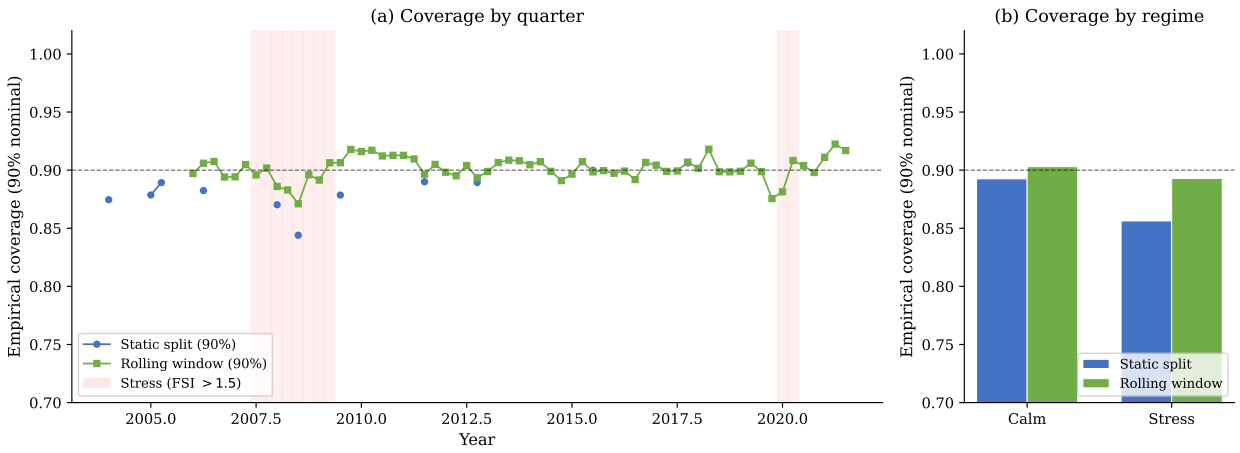
Notes: Empirical coverage against nominal coverage for three conformal methods: static split (calibrating once on 11 fixed validation quarters), locally adaptive (heteroskedastic intervals via residual normalization), and rolling window (recalibrating on the preceding 8 quarters before each evaluation quarter). The dashed line indicates perfect calibration.

Figure 10: **Adaptive interval width and per-decile coverage**



Notes: Locally-adaptive conformal intervals at 90% nominal coverage. Panel A shows mean interval width by decile of $|\widehat{y}|$. Panel B shows per-decile empirical coverage; bars below the dashed 90% line are highlighted.

Figure 11: **Coverage robustness: time series and stress regimes**



Notes: Panel A: per-quarter empirical coverage at 90% nominal for static split and rolling-window conformal. Shaded regions indicate stress quarters (FSI > 1.5). Panel B: coverage by financial regime (calm vs. stress) for both methods. The rolling window achieves near-nominal coverage in both regimes.

to both cross-sectional dependencies and distributional shifts over time, the formal exchangeability assumption may not hold exactly; we therefore treat conformal prediction as a distribution-free calibration device and evaluate coverage validity empirically.[13]

We partition the data into training, calibration, and held-out test sets. For each calibration pair $(i, a) \in \mathcal{I}_{\text{cal}}$, we compute the absolute residual $s_{ia} = |y_{ia,t+1} - \widehat{y}_{ia,t+1}|$ and construct the split conformal interval $C_{1-\alpha} = [\widehat{y}_{ia,t+1} \pm \widehat{q}_{1-\alpha}]$, where $\widehat{q}_{1-\alpha}$ is the appropriate quantile of the calibration scores.[14] We report three variants: a static split calibrating once on 11 validation quarters; a locally adaptive variant that normalizes residuals by the local median absolute deviation within deciles of $|\widehat{y}_{ia,t+1}|$ to produce heteroskedastic intervals (Lei et al., 2018); and a rolling window variant that recalibrates on the preceding 8 quarters before each evaluation quarter, trading fixed calibration for adaptivity to distributional drift.

Figure 9 reports empirical coverage for the estimated prediction intervals against nominal coverage. At the 95% level, all three methods track the nominal level closely. The key difference emerges at 90%: the static split exhibits mild under-coverage, consistent with distributional shift, while rolling-window recalibration tracks the nominal level more accurately. Figure 11 examines coverage stability across time and regimes at 90% nominal. The rolling window achieves coverage ranging from 88.6% to 91.6% across all evaluated quarters. The static split shows a calm-stress gap (88.9% vs. 86.9%), which the rolling window largely closes (90.3% vs. 89.9%), showing near-uniformity across regimes.[15]

[13] Extensions to covariate-shift conformal methods (Tibshirani et al., 2019) and conformal procedures for dependent data (Barber et al., 2023; Chernozhukov et al., 2018) are a natural direction for future work.

[14] Specifically, $\widehat{q}_{1-\alpha}$ is the $\lceil (n+1)(1-\alpha) \rceil / n$ quantile of $\{s_{ia}\}$ and $n = |\mathcal{I}_{\text{cal}}|$.

[15] Importantly, we note that these are marginal coverage rates pooled across all investor-asset pairs (i, a)

4 A Theory of Optimal Policy with Predictive Models

The empirical results in the preceding sections demonstrate that graph-based predictive models can accurately forecast institutional trading and recover economically meaningful measures of systemic risk. These objects are of independent interest for financial stability monitoring. We now develop a tractable equilibrium model of fire sales and optimal macroprudential intervention that provides a framework for interpreting the policy and welfare value of the empirical forecasts from the preceding sections. We show that even in an environment subject to the usual Lucas critique, high-dimensional predictive models have value to the regulator by allowing for better cross-sectional policy targeting. The theory does not imply that the predictive model by itself identifies policy counterfactuals. Instead, it clarifies a division of labor: structural knowledge governs the effect of policy instruments, while the predictive model estimates the high-dimensional cross-sectional targeting statistics that enter the policy rule.

4.1 Setup

Time is discrete, $t = 1, 2$. There are N assets. There are I intermediary types, each of equal measure, with a representative intermediary of each type i. There is also a representative arbitrageur. For simplicity in the main text, intermediaries start date $t = 1$ with an inherited portfolio of assets. In Appendix D, we introduce a date 0 in which intermediaries optimally choose asset allocations, and study implications for optimal regulation.

At date 1, intermediaries face binding constraints that force them to sell assets prior to maturity to arbitrageurs, who are second best users. At date 2, payoffs are distributed and consumption occurs. We assume that at date 1, intermediaries and arbitrageurs know the true values of all underlying parameters. The regulator's information structure will be introduced below.

Intermediaries. Intermediaries are risk neutral. Intermediaries enter date 1 with a vector $q_i = (q_{i1}, \ldots, q_{iN})^T$ of asset positions. If $q_{in} < 0$, then intermediary i has undertaken a negative investment (shorting) asset n. If held to maturity, intermediary i's holdings of asset n will produce a (stochastic) per-unit return R_{in} at date 2. We denote $R_i = (R_{i1}, \ldots, R_{iN})^T$ to be the vector of asset returns.

At date 1, intermediary i can sell assets prior to maturity. We denote $\ell_{in} \geq 0$ to be sales by intermediary i at endogenous price γ_n, with $\ell_i = (\ell_{i1}, \ldots, \ell_{iN})^T$ and $\gamma = (\gamma_1, \ldots, \gamma_N)^T$. Intermediary i faces an adjustment cost $\frac{1}{2}\ell_i^T H_i^\ell \ell_i$ on asset sales, where H_i^ℓ is $N \times N$. Assets will be sold at a discount on their fundamental value ($\gamma \leq R_i$, see below), and intermediary i faces a set of "rollover

within each quarter. Conditional coverage for specific investor types, asset classes, or individual entities may of course differ. Figure 10 provides partial evidence: locally-adaptive intervals at 90% nominal show coverage by decile of $|\widehat{y}_{ia,t+1}|$ that is approximately uniform, though the lowest deciles fall to roughly 83%, indicating that positions with the smallest predicted trades have somewhat less reliable intervals.

constraints" that force asset sales. This set of M constraints is given by

$$A_i^q q_i + \rho_i \leq A_i^\ell \ell_i, \tag{12}$$

where A_i^q, A_i^ℓ are $M \times N$ and ρ_i is $M \times 1$. For example, equation 12 can capture constraints on asset positions (e.g., a limit on debt) or a requirement to raise funds based on asset holdings (e.g., a cost of maintaining the project).[16]

At date 2, intermediary i realizes payoff on assets held to maturity and consumes. Intermediary i's total payoff (consumption) at date 2, inclusive of adjustment costs, is

$$U_i = q_i^T R_i - \ell_i^T (R_i - \gamma) - \frac{1}{2} \ell_i^T H_i^\ell \ell_i. \tag{13}$$

Arbitrageurs. A representative arbitrageur is a second-best user of intermediary assets. If the arbitrageur purchases a vector $L = (L_1, \ldots, L_N)^T$ of intermediary assets at date 1, the arbitrageur can use them in a production technology to produce $\mathcal{F}(L) = L^T \overline{\gamma} - \frac{1}{2} L^T \Gamma L$ units of the consumption good at date 2, where $\overline{\gamma}$ is $N \times 1$ and Γ is $N \times N$. The representative arbitrageur's payoff is

$$U_A = L^T (\overline{\gamma} - \gamma) - \frac{1}{2} L^T \Gamma L. \tag{14}$$

Market Clearing. The market for liquidations of each asset must clear at date 1, that is,

$$L = \sum_i \ell_i, \tag{15}$$

which specifies N market clearing conditions (one for each asset n).

Competitive Equilibrium. We define a competitive equilibrium as follows.

Definition 1. *A competitive equilibrium of the model is a vector of prices γ and a set of allocations $\{\ell_i, L\}$ such that:*

1. *Intermediary i chooses ℓ_i to maximize utility (equation 13) subject to the rollover constraint (12), taking prices γ as given.*
2. *Arbitrageurs choose L maximize utility (equation 14), taking prices γ as given.*
3. *The liquidation markets clear (equation 15).*

[16] We simplify analysis by not having equation 12 depend on the liquidation price γ, as for example in price-dependent collateral constraints. This enables us to maintain a linear-quadratic structure throughout the paper. It is straightforward to extend analysis to include prices in constraints, but the characterization of the ex-ante optimal portfolio would no longer admit a closed-form solution.

4.2 Regulator's Model Design and Intervention

At date 1, the regulator can intervene in order to try to manage the fire sale price impact of liquidations. Formally, we assume that the regulator can impose a vector $\tau_i = (\tau_{i1}, \ldots, \tau_{iN})^T$ of revenue-neutral liquidation wedges on each intermediary i, which alter the intermediary's perceived price for selling the asset.[17] The wedge τ_{in} is formally a revenue-neutral tax on intermediary i from selling asset n, with $\tau_{in} < 0$ being a subsidy for sale.[18] As a result, intermediary i's payoff at date 2 is modified to be

$$U_i - (\ell_i^T - \ell_i^{*T})\tau_i \tag{16}$$

where $\ell_i^{*T}\tau_i$ is equilibrium revenue remissions to intermediary i based on the equilibrium asset liquidations ℓ_i^* of intermediaries of type i. Intermediaries take revenue remissions as given. We allow for the possibility that the regulator has incomplete instruments, represented by a regulatory cost $\delta(\tau) = \frac{1}{2}\tau^T\Delta\tau$, where Δ is $NI \times NI$.[19] To simplify the exposition, we introduce an assumption of matrix symmetry that we maintain throughout the paper.

Assumption 1. *The matrices H_i^ℓ, Γ, Δ are symmetric.*

Information Structure and Timing. In contrast to private agents, the regulator does not know the true values of the parameters $\Phi = \{A_i^q, A_i^\ell, H_i^\ell, \rho_i, R_i, \overline{\gamma}\}$. That is, the regulator is uncertain as to the true parameters underlying the rollover constraint (equation 12), the asset return R_i, the arbitrageurs' baseline productivity $\overline{\gamma}$, and the liquidation adjustment cost H_i^ℓ. We denote the regulator's prior to be $\Phi \sim \mu_0$.[20]

Before setting wedges, the regulator can use a *model* to make an inference about the true parameters. Formally, a model $M \in \mathcal{M}$ is a process of drawing a signal s of the parameters Φ. When the regulator draws a signal s from running model M, the regulator's posterior distribution is given by $\Phi \sim \mu_p|s, M$. After running the model and drawing the signal, the regulator chooses its wedges τ. After the regulator chooses its wedges, private agents move and the equilibrium is

[17] In Appendix D.4, we instead assume the regulator must use asset holding subsidies rather than liquidation taxes. The results at date 1 are identical, but the asset holding subsidies can give rise to additional moral hazard at date 0 when asset allocations q are chosen.

[18] Due to its flexibility, the wedge approach is commonly employed in the macroprudential policy literature (Farhi and Werning 2016). Wedges can be interpreted as taxes and also as quantity restrictions (e.g., Clayton and Schaab 2022).

[19] One could instead model incompleteness as a restriction $\Delta(\tau) \leq 0$, which will imply a shadow cost on the regulatory incompleteness constraint measured by the Lagrange multiplier λ. This shadow cost is akin to the reduced-form cost function $\delta(\tau) = \lambda\Delta(\tau)$ except that λ is endogenous.

[20] Assuming that private agents are perfectly informed is a simplifying assumption. Assuming that Γ is known to the regulator simplifies the analysis by eliminating the ability of a regulator to learn about the price impact of liquidations from observing a signal of γ or ℓ. This will allow us to fully separate predictive and causal channels in our framework. Absent this assumption, predictive models that inform a regulator about γ and ℓ might have even more value because they would also allow the regulator to learn about these structural parameters that determine the causal impact of a policy intervention (even if very little information is learned).

determined. Because the regulator sets wedges before the equilibrium is determined, the regulator cannot obtain any new information from observing the market before setting regulation.

4.2.1 Equilibrium Outcome for Given Wedges

We solve the regulator's optimum by first characterizing the equilibrium outcome, given the regulator's wedges $\tau = (\tau_1^T, \ldots, \tau_I^T)^T$ on the equilibrium at date 1. Our model is substantially simplified by the information structure: because private agents directly observe Φ, private agents do not learn from the regulator's choice of model or the signal drawn. As a result, the realized equilibrium outcome depends on the wedges τ and the true model parameters Φ, but not (for a given vector of asset allocations $q = (q_1^T, \ldots, q_I^T)^T$) on the regulator's choice of model M or the realized signal s.

The linear-quadratic structure of preferences and the rollover constraint leads to a characterization of the equilibrium as a simple linear system of equations. The following Lemma characterizes this equilibrium.

Lemma 1. *Given regulatory wedges τ, the equilibrium at date 1 is given by*

$$\ell_i = \overline{\ell}_i + \Lambda_i^q q_i - \Lambda_i^\tau \tau_i - \sum_{j=1}^{N} \left[\Lambda_j^{q,e} q_j^* - \Lambda_j^{\tau,e} \tau_j^* \right] \tag{17}$$

$$\gamma = \overline{\gamma} - \Gamma \sum_i \ell_i \tag{18}$$

where $\overline{\ell}_i$ $(N \times 1)$ and the loadings $\Lambda_i^q, \Lambda_i^\tau, \Lambda_i^{q,e}, \Lambda_i^{\tau,e}$ $(N \times N)$ are defined in the proof.

The characterization of the equilibrium in Lemma 1 is intuitive. Liquidations start from a baseline level $\overline{\ell}_i$ and increase (for positive loadings Λ_i^q) in asset holdings while decreasing (for positive loadings Λ_i^τ) in the liquidation wedge. Higher liquidations result in a lower liquidation price (for positive Γ) due to more assets having to be absorbed by arbitrageurs (equation 18). This means that liquidations by intermediary i decrease in asset holdings and increase in the liquidation wedges applied to other intermediaries within the same sector and across different sectors (for positive matrix loadings), a result of a substitution effect resulting from the increase in equilibrium price. In a model without fire sales, the loadings satisfy $\Lambda_j^{q,e} = \Lambda_j^{\tau,e} = 0$. We distinguish in equation 17 between the asset choices of intermediary i and the wedges applied to intermediary i's liquidations (denoted with no $*$) as opposed to equilibrium objects (denoted with $*$) that enter because they determine the equilibrium liquidation price.

Crucially, given the information structure that private agents have a finer information partition than the regulator, the regulator's model choice can alter the endogenous portfolios q_i that feed into the determination of the equilibrium liquidations and liquidation prices through choice of the regulatory wedges (see Appendix D), but not by changing the structural loadings (or agents' beliefs about them) $\Lambda_i = \{\Lambda_i^q, \Lambda_i^\tau, \Lambda_i^{q,e}, \Lambda_i^{\tau,e}\}$ that translate portfolio quantities and wedges into outcomes.

In this sense, the equilibrium determination and the regulator's forecasting problem satisfy a key form of policy invariance.

The assumption that private agents observe the full state at date 1 can be weakened substantially. It is enough that any regulator-generated public information be informative only about the predictive component of the state—the baseline pattern of liquidation pressure—and not about the transmission component that determines how portfolios and policy wedges map into equilibrium liquidations and prices. Under Bayesian updating, private agents may learn from the regulator about where fire-sale pressure is likely to concentrate, while the structural loadings that govern the causal effect of intervention remain unchanged. In that case, the regulator's model choice affects equilibrium only through the posterior-predictive no-intervention liquidation vector, and the policy invariance result continues to hold. Appendix D.5 formalizes this extension.

4.3 Regulator's Optimal Wedges

We solve the regulator's problem by backward induction: first, we characterize the regulator's optimal wedges τ, given a choice of model M and a realized signal s. We then characterize the regulator's welfare given model choice M in terms of sufficient statistics.[21] To simplify analysis, we assume that the regulator places equal weight on all intermediaries but places a welfare weight of zero on arbitrageurs.[22]

Given that liquidation wedges are revenue-neutral, the regulator's optimal choice of τ solves

$$\max_{\tau} \mathbb{E}\left[\sum_i U_i \,\middle|\, s, M\right] - \delta(\tau),$$

subject to equilibrium determination (Lemma 1).

As preliminaries to the proposition below, we define $\overline{\ell}_i(q) = \overline{\ell}_i + \Lambda_i^q q_i - \sum_i \Lambda_i^{q,e} q_i$ to be the $N \times 1$ vector of liquidations by intermediary i of each asset if there is no regulatory intervention ($\tau = 0$). We define $L(q) = \sum_i \overline{\ell}_i(q)$ to be the $N \times 1$ vector capturing total liquidations of each asset (across all intermediaries) if there is no intervention. The following proposition characterizes the regulator's optimal liquidation wedges in terms of these objects and model parameters.

Proposition 1. *Given a model M and signal s, the regulator's optimal wedges are*

$$\tau^* = \mathbb{E}\left[\Xi \,\middle|\, s, M\right]^{-1} \mathbb{E}\left[(\sum_i \overline{\Lambda}_i^{\tau})^T \Gamma L(q) \,\middle|\, s, M\right] \tag{19}$$

where $\Xi = \overline{\Lambda}^{\tau T} + (\sum_i \overline{\Lambda}_i^{\tau})^T \Gamma (\sum_i \overline{\Lambda}_i^{\tau}) + \Delta$, where $\overline{\Lambda}_i^{\tau} = (e_i \otimes I_N)^T \Lambda_i^{\tau} - (\Lambda_1^{\tau,e}, \ldots, \Lambda_I^{\tau,e})$ is $N \times NI$ (where e_i is the standard basis vector whose i^{th} element is 1 and $\otimes$ is the Kronecker product), and

[21] In Appendix D, we study the regulator's optimal choice of model.

[22] This focuses attention on a distributive externality from shifting wealth between arbitrageurs and intermediaries, who effectively have different marginal values of wealth at date 1 (Dávila and Korinek 2017).

where $\overline{\Lambda}^{\tau} = (\overline{\Lambda}_1^{\tau T}, \ldots, \overline{\Lambda}_I^{\tau T})^T$ *is* $NI \times NI$.

The optimal wedges of Proposition 1 are familiar from the macroprudential policy literature on fire sales, and intuitively encode an expected marginal cost-marginal benefit trade-off. The marginal cost of the policy is captured in the (conditional expectation of the) inverse matrix Ξ, while the marginal benefit is captured in the expectation.

There are three components to the private and regulatory marginal cost of liquidations, reflecting the distortion of intermediaries' activities away from their private optimum. First, increasing liquidation wedges directly distorts the intermediaries' activities (the first term of Ξ). Second, by using wedges to alter equilibrium prices, the regulator changes the incentives for intermediaries to sell different assets (the second term). Finally, there is the regulatory cost Δ.

The social marginal benefit of regulation arises from the mitigation of the fire sale. This has two components that are central to our analysis. First is the causal effect of the policy intervention on equilibrium liquidation prices, captured by the term $(\sum_i \overline{\Lambda}_i^{\tau})^T \Gamma$. The utility consequence of these price changes is proportional to the total value of assets being sold by intermediaries, $L(q)$.

Importantly, this means the social benefit of regulation derives from a product of the causal impact of the policy intervention, $(\sum_i \overline{\Lambda}_i^{\tau})^T \Gamma^T$, and the social value of changing the price, here given by $L(q)$. This means that in designing regulation, there is value not only to identifying causal policy impacts, but also to predicting the magnitude of liquidations $L(q)$. To fully disentangle these two mechanisms, we can assume independence of the predictive and causal components of the system.[23]

Definition 2 (Predictive-Causal Independence)**.** *We have predictive-causal independence if* $\{\overline{\Lambda}_i^{\tau}\}$ *and* $\{\bar{\ell}_i, \Lambda_i^q, \Lambda_i^{q,e}\}$ *are independent of one another.*

Under predictive-causal independence, we obtain the following corollary to Proposition 1.

Corollary 1. *Under predictive-causal independence, the regulator's optimal wedges are*

$$\tau^* = \mathbb{E}\left[\Xi \middle| s, M\right]^{-1} \underbrace{\mathbb{E}\left[(\sum_i \overline{\Lambda}_i^{\tau})^T \Gamma \middle| s, M\right]}_{\text{Causal: Policy Impact on Liquidation Price}} \overbrace{\mathbb{E}\left[L(q) \middle| s, M\right]}^{\text{Predictive: Total Liquidations}} \tag{20}$$

An important implication of Proposition 1 and Corollary 1 is that a model that is purely predictive—that is, that can predict liquidations $L(q)$—can be valuable to a regulator, provided that the regulator has some prior or posterior knowledge over the causal impact of the policy. This causal component of the optimal policy rule could be obtained through a fully-specified equilibrium structural model (e.g., as reviewed in Christiano et al. 2005) or, under certain conditions, from

[23] Naturally absent this assumption, we could perform an analogous decomposition to Corollary 1, but also include the covariance between the two terms.

causal effects that are estimated empirically in reduced form (Guren et al. 2021; McKay and Wolf 2023; Caravello et al. 2025). The predictive information informs the regulator as to the magnitude and margins for intervention by informing the regulator about the social benefit of the intervention. Corollary 1 implies that, holding fixed the causal impact of the policy, the regulator would design larger-magnitude interventions when the regulator's model predicted that total liquidations would be larger.

Formally, we will define a predictive model to be a model that delivers information only on the predictive component of Corollary 1.

Definition 3. *We say a model M is* predictive *if, under predictive-causal independence, the posterior joint distribution of $\{\overline{\Lambda}_i^T\}$ is the same as the prior for all signals s.*

4.4 Predictive Accuracy and Welfare

We next ask what the welfare benefit to a regulator at date 1 is based on the model M the regulator runs.[24] Intuitively, for a predictive model, Proposition 1 suggests that the welfare gains obtained from using the model should be related to the predictive accuracy of that model. In this section, we formalize this intuition, showing that the predictive correlation of a predictive model's forecasts—weighted appropriately according to the causal leverage of the policy—is a sufficient statistic for the welfare gains from the model.

As a preliminary to the proposition below, we define a few objects. Given a square matrix W, we define variance and covariance operators that use W as a weighting matrix:

$$\mathrm{Cov}_W(X,Y) = \mathbb{E}\left[(X - E[X])^T W (Y - E[Y])\right], \quad \mathrm{Var}_W(X) = \mathrm{Cov}_W(X,X).$$

The maximum ex-ante expected welfare gain (relative to relying on the prior) within the class of predictive models, $\Delta V_{\max}$, is attained by a perfect predictive signal—that is, a predictive model M whose forecasts $\widehat{L}(q) = \mathbb{E}\left[L(q) \mid s, M\right]$ satisfy $\widehat{L}(q) = L(q)$. The following proposition characterizes welfare losses relative to the perfect forecast benchmark $\Delta V_{\max}$ in terms of the model's predictive accuracy.

Proposition 2. *Under predictive-causal independence, the regulator's expected welfare gain from employing a predictive model M, relative to relying on the prior, is*

$$\Delta V(M) = \Delta V_{\max} \cdot \rho^2_{\Theta_0}(M), \tag{21}$$

where

$$\rho_{\Theta_0}(M) \equiv \frac{\mathrm{Cov}_{\Theta_0}(L, \widehat{L})}{\sqrt{\mathrm{Var}_{\Theta_0}(L)\,\mathrm{Var}_{\Theta_0}(\widehat{L})}},$$

[24] In Appendix D, we consider how the regulator's model choice affects intermediaries' optimal portfolio allocations when they are originally chosen.

where the weighting matrix Θ_0 *is given* $\Theta_0 = \mathbb{E}_0[\Upsilon^T \Psi \Upsilon | M]$, *where* $\Psi = \mathbb{E}_0[2(\sum_i \overline{\Lambda}_i^\tau)^T \Gamma (\sum_i \overline{\Lambda}_i^\tau) + \Delta + \overline{\Lambda}^{\tau T} H^\ell \overline{\Lambda}^\tau]$, *and where* $\Upsilon = (\mathbb{E}_0[\Xi])^{-1} \mathbb{E}_0[(\sum_i \overline{\Lambda}_i^\tau)^T \Gamma]$.

Proposition 2 shows that the welfare gains from a predictive model scale linearly with the Θ_0-weighted R-squared achieved by the model in predicting liquidations. The weighting matrix Θ_0 has a natural interpretation as the metric that converts variation in predicted liquidations $\hat{L}(q)$ into variation in welfare after the regulator applies the optimal wedges τ^*: therefore, assets that generate larger externalities or for which the intervention has a higher causal leverage on outcomes receive a larger weight in the statistic $\rho_{\Theta_0}(M)$. The predictive R-squared has in fact an exact interpretation as the fraction of the maximum achievable welfare gain within the class of predictive models that is actually attained. This sufficient statistic provides a direct way to map the empirical performance of predictive models to welfare.

Proposition 2 completes the characterization of the regulator's ex-post problem. In Appendix D.2, we study the equilibrium feedback of model choice and ex-post intervention on intermediaries' ex-ante portfolio decisions. The preceding empirical sections demonstrate that high-dimensional predictive models can deliver accurate cross-sectional forecasts of trading behavior—the targeting statistics that this framework suggests have welfare value.

5 Conclusion

This paper asks whether the combination of granular portfolio holdings data and modern deep learning methods can improve financial regulation, and provides evidence that it can. We show that the network structure of portfolio holdings contains far more information about fire-sale vulnerability than conventional low-dimensional summaries capture, and we introduce a graph-based deep learning architecture that recovers it in an economically interpretable way. The graph transformer learns latent representations of investors and assets that deliver strong out-of-sample conditional forecasts of trading behavior including during crisis episodes, that explain the cross-section of asset price dislocations during stress events with more than ten times the explanatory power of existing approaches, and that outperform conventional institution-level systemic risk metrics. Our complementary theoretical framework clarifies why these predictive objects have welfare value: they provide a practical way to estimate the sufficient statistics that govern the cross-sectional targeting of policy interventions. More broadly, the paper suggests a division of labor between prediction and structure in policy problems with high-dimensional state spaces. Predictive models are not substitutes for structural analysis or causal inference, but they can be powerful complements: their role is to recover the heterogeneity that structural models need for accurate targeting but struggle to capture on their own. As AI methods continue to advance and regulatory data grows richer, this complementarity is likely to become increasingly important for policy design.

References

Acemoglu, Daron, Asuman Ozdaglar, and Alireza Tahbaz-Salehi, "Systemic risk and stability in financial networks," *American Economic Review*, 2015, *105* (2), 564–608.

Acharya, Viral V, Lasse H Pedersen, Thomas Philippon, and Matthew Richardson, "Measuring systemic risk," *The review of financial studies*, 2017, *30* (1), 2–47.

Adrian, Tobias and Hyun Song Shin, "Procyclical leverage and value-at-risk," *The Review of Financial Studies*, 2014, *27* (2), 373–403.

Adrian, Tobias and Markus K Brunnermeier, "CoVaR," *The American Economic Review*, 2016, *106* (7), 1705.

Angelopoulos, Anastasios N and Stephen Bates, "Conformal Prediction: A Gentle Introduction," *Foundations and Trends in Machine Learning*, 2023, *16* (4), 494–591.

Aramonte, Sirio, Andreas Schrimpf, and Hyun Song Shin, "Non-bank financial intermediaries and financial stability," *BIS Working Paper*, 2023.

Athey, Susan, "Beyond prediction: Using big data for policy problems," *Science*, 2017, *355* (6324), 483–485.

Athey, Susan, "The impact of machine learning on economics," in "The economics of artificial intelligence: An agenda," University of Chicago Press, 2018, pp. 507–547.

Athey, Susan and Guido W Imbens, "Machine learning methods that economists should know about," *Annual Review of Economics*, 2019, *11* (1), 685–725.

Athey, Susan and Stefan Wager, "Policy learning with observational data," *Econometrica*, 2021, *89* (1), 133–161.

Barber, Rina Foygel, Emmanuel J. Candès, Aaditya Ramdas, and Ryan J. Tibshirani, "Conformal Prediction Beyond Exchangeability," *The Annals of Statistics*, 2023, *51* (2), 816–845.

Barro, Robert J and David B Gordon, "A positive theory of monetary policy in a natural rate model," *Journal of political economy*, 1983, *91* (4), 589–610.

Benoit, Sylvain, Jean-Edouard Colliard, Christophe Hurlin, and Christophe Pérignon, "Where the Risks Lie: A Survey on Systemic Risk," *Review of Finance*, 2017, *21* (1), 109–152.

Bernanke, Ben S and Mark Gertler, "Agency costs, collateral, and business fluctuations," 1986.

Bianchi, Javier, "Overborrowing and Systemic Externalities in the Business Cycle," *American Economic Review*, December 2011, *101* (7), 3400–3426.

Bianchi, Javier, "Efficient Bailouts?," *American Economic Review*, December 2016, *106* (12), 3607–59.

Bianchi, Javier and Enrique G. Mendoza, "Optimal Time-Consistent Macroprudential Policy," *Journal of Political Economy*, 2018, *126* (2), 588–634.

Bouchaud, Jean-Philippe, Julius Bonart, Jonathan Donier, and Martin Gould, *Trades, Quotes and Prices: Financial Markets Under the Microscope*, Cambridge University Press, 2018.

Brainard, William C and James Tobin, "Pitfalls in financial model building," *The American*

economic review, 1968, *58* (2), 99–122.

Brownlees, Christian and Robert F Engle, "SRISK: A Conditional Capital Shortfall Measure of Systemic Risk," *The Review of Financial Studies*, 2017, *30* (1), 48–79.

Brunnermeier, Markus K and Martin Oehmke, "Bubbles, financial crises, and systemic risk," *Handbook of the Economics of Finance*, 2013, *2*, 1221–1288.

Bryzgalova, Svetlana, Victor DeMiguel, Sicong Li, and Markus Pelger, "Asset-pricing factors with economic targets," *Available at SSRN*, 2023, *4344837*.

Bybee, J Leland, "The ghost in the machine: Generating beliefs with large language models," *Working Paper*, 2025.

Caballero, Ricardo J. and Arvind Krishnamurthy, "International and domestic collateral constraints in a model of emerging market crises," *Journal of Monetary Economics*, December 2001, *48* (3), 513–548.

Caravello, Tomás, Alisdair McKay, and Christian Wolf, "Evaluating Monetary Policy Counterfactuals:(When) Do We Need Structural Models?," *Working Paper*, 2025.

Chari, V. V. and Patrick J. Kehoe, "Bailouts, Time Inconsistency, and Optimal Regulation: A Macroeconomic View," *American Economic Review*, September 2016, *106* (9), 2458–93.

Chen, Hui, Yuhan Cheng, Yanchu Liu, and Ke Tang, "Teaching economics to the machines," *Available at SSRN 4642167*, 2023.

Chen, Luyang, Markus Pelger, and Jason Zhu, "Deep learning in asset pricing," *Management Science*, 2024, *70* (2), 714–750.

Chen, Qi, Itay Goldstein, and Wei Jiang, "Payoff complementarities and financial fragility: Evidence from mutual fund outflows," *Journal of financial economics*, 2010, *97* (2), 239–262.

Chernozhukov, Victor, Kaspar Wüthrich, and Yinchu Zhu, "Exact and Robust Conformal Inference Methods for Predictive Machine Learning with Dependent Data," *Proceedings of the 31st Conference on Learning Theory*, 2018, *75*, 732–749.

Chevalier, Judith and Glenn Ellison, "Risk taking by mutual funds as a response to incentives," *Journal of political economy*, 1997, *105* (6), 1167–1200.

Christiano, Lawrence J, Martin Eichenbaum, and Charles L Evans, "Nominal rigidities and the dynamic effects of a shock to monetary policy," *Journal of political Economy*, 2005, *113* (1), 1–45.

Clayton, Christopher and Andreas Schaab, "Multinational Banks and Financial Stability," *The Quarterly Journal of Economics*, 01 2022, *137* (3), 1681–1736.

Clayton, Christopher and Andreas Schaab, "Bail-Ins, Optimal Regulation, and Crisis Resolution," *The Review of Financial Studies*, 03 2025, p. hhaf002.

Cohen, Lauren, Yiwen Lu, and Quoc H Nguyen, "Mimicking Finance," *Working Paper*, 2026.

Coppola, Antonio, "In safe hands: The financial and real impact of investor composition over the credit cycle," *The Review of Financial Studies*, 2025, p. hhaf017.

Coval, Joshua and Erik Stafford, "Asset fire sales (and purchases) in equity markets," *Journal*

of Financial Economics, 2007, *86* (2), 479–512.

Derrow-Pinion, Austin, Jennifer She, David Wong, Oliver Lange, Todd Hester, Luis Perez, Marc Nunkesser, Seongjae Lee, Xueying Guo, Brett Wiltshire et al., "Eta prediction with graph neural networks in google maps," in "Proceedings of the 30th ACM international conference on information & knowledge management" 2021, pp. 3767–3776.

Devlin, Jacob, Ming-Wei Chang, Kenton Lee, and Kristina Toutanova, "Bert: Pre-training of deep bidirectional transformers for language understanding," in "Proceedings of the 2019 conference of the North American chapter of the association for computational linguistics: human language technologies, volume 1 (long and short papers)" 2019, pp. 4171–4186.

Dick-Nielsen, Jens, "How to clean enhanced TRACE data," *Available at SSRN 2337908*, 2014.

Dolphin, Rian, Barry Smyth, and Ruihai Dong, "Stock embeddings: Learning distributed representations for financial assets," *arXiv preprint arXiv:2202.08968*, 2022.

Dávila, Eduardo and Anton Korinek, "Pecuniary Externalities in Economies with Financial Frictions," *The Review of Economic Studies*, 02 2017, *85* (1), 352–395.

Einav, Liran and Jonathan Levin, "The data revolution and economic analysis," *Innovation Policy and the Economy*, 2014, *14* (1), 1–24.

Einav, Liran and Jonathan Levin, "Economics in the age of big data," *Science*, 2014, *346* (6210), 1243089.

Elenev, Vadim, Tim Landvoigt, and Stijn Van Nieuwerburgh, "A Macroeconomic Model with Financially Constrained Producers and Intermediaries," *Econometrica*, 2021, *89* (3), 1361–1418.

Elliott, Matthew, Benjamin Golub, and Matthew O Jackson, "Financial networks and contagion," *American Economic Review*, 2014, *104* (10), 3115–3153.

Fang, Xiang, Bryan Hardy, and Karen K Lewis, "Who holds sovereign debt and why it matters," *The Review of Financial Studies*, 2025, p. hhaf031.

Farboodi, Maryam and Laura Veldkamp, "Long-run growth of financial data technology," *American Economic Review*, 2020, *110* (8), 2485–2523.

Farhi, Emmanuel and Iván Werning, "A theory of macroprudential policies in the presence of nominal rigidities," *Econometrica*, 2016, *84* (5), 1645–1704.

Faria-e Castro, Miguel, Joseba Martinez, and Thomas Philippon, "Runs versus lemons: Information disclosure and fiscal capacity," *The Review of Economic Studies*, 2017, *84* (4), 1683–1707.

Fisher, Irving, "The debt-deflation theory of great depressions," *Econometrica: Journal of the Econometric Society*, 1933, pp. 337–357.

Fontanier, Paul, "Optimal policy for behavioral financial crises," *Journal of Financial Economics*, 2025, *166*, 104005.

Friedman, Milton, "The methodology of positive economics," *Essays In Positive Economics*, 1953.

Fuster, Andreas, Paul Goldsmith-Pinkham, Tarun Ramadorai, and Ansgar Walther, "Predictably unequal? The effects of machine learning on credit markets," *The Journal of Finance*,

2022, *77* (1), 5–47.

Gabaix, Xavier, Ralph SJ Koijen, Robert Richmond, and Motohiro Yogo, "Asset embeddings," *Available at SSRN 4507511*, 2024.

Gabaix, Xavier, Ralph SJ Koijen, Robert Richmond, and Motohiro Yogo, "Upgrading Credit Pricing and Risk Assessment through Embeddings," *Available at SSRN*, 2025.

Giglio, Stefano, Bryan Kelly, and Dacheng Xiu, "Factor models, machine learning, and asset pricing," *Annual Review of Financial Economics*, 2022, *14* (1), 337–368.

Gillis, Talia B and Jann L Spiess, "Big data and discrimination," *The University of Chicago Law Review*, 2019, *86* (2), 459–488.

Goldstein, Itay and Yaron Leitner, "Stress tests and information disclosure," *Journal of Economic Theory*, 2018, *177*, 34–69.

Goldstein, Itay, Hao Jiang, and David T Ng, "Investor flows and fragility in corporate bond funds," *Journal of Financial Economics*, 2017, *126* (3), 592–613.

Gu, Shihao, Bryan Kelly, and Dacheng Xiu, "Empirical asset pricing via machine learning," *The Review of Financial Studies*, 2020, *33* (5), 2223–2273.

Gu, Shihao, Bryan Kelly, and Dacheng Xiu, "Autoencoder asset pricing models," *Journal of Econometrics*, 2021, *222* (1), 429–450.

Guren, Adam, Alisdair McKay, Emi Nakamura, and Jón Steinsson, "What do we learn from cross-regional empirical estimates in macroeconomics?," *NBER Macroeconomics Annual*, 2021, *35* (1), 175–223.

Haddad, Valentin, Alan Moreira, and Tyler Muir, "When selling becomes viral: Disruptions in debt markets in the COVID-19 crisis and the Fed's response," *The Review of Financial Studies*, 2021, *34* (11), 5309–5351.

Hamilton, Will, Zhitao Ying, and Jure Leskovec, "Inductive representation learning on large graphs," *Advances in neural information processing systems*, 2017, *30*.

He, Kaiming, Xinlei Chen, Saining Xie, Yanghao Li, Piotr Dollár, and Ross Girshick, "Masked Autoencoders Are Scalable Vision Learners," in "Proceedings of the IEEE/CVF Conference on Computer Vision and Pattern Recognition" 2022, pp. 16000–16009.

Hendrycks, Dan and Kevin Gimpel, "Gaussian error linear units (gelus)," *arXiv preprint arXiv:1606.08415*, 2016.

Jiang, Dejun, Zhenxing Wu, Chang-Yu Hsieh, Guangyong Chen, Ben Liao, Zhe Wang, Chao Shen, Dongsheng Cao, Jian Wu, and Tingjun Hou, "Could graph neural networks learn better molecular representation for drug discovery? A comparison study of descriptor-based and graph-based models," *Journal of cheminformatics*, 2021, *13*, 1–23.

Jumper, John, Richard Evans, Alexander Pritzel, Tim Green, Michael Figurnov, Olaf Ronneberger, Kathryn Tunyasuvunakool, Russ Bates, Augustin Žídek, Anna Potapenko et al., "Highly accurate protein structure prediction with AlphaFold," *nature*, 2021, *596* (7873), 583–589.

Kindleberger, Charles and Robert Aliber, *Manias, panics and crashes: a history of financial*

crises, Springer, 1978.

Kingma, Diederik P, "Adam: A method for stochastic optimization," *arXiv preprint arXiv:1412.6980*, 2014.

Kiyotaki, Nobuhiro and John Moore, "Credit cycles," *Journal of political economy*, 1997, *105* (2), 211–248.

Kleinberg, Jon, Himabindu Lakkaraju, Jure Leskovec, Jens Ludwig, and Sendhil Mullainathan, "Human decisions and machine predictions," *The quarterly journal of economics*, 2018, *133* (1), 237–293.

Kleinberg, Jon, Jens Ludwig, Sendhil Mullainathan, and Ziad Obermeyer, "Prediction policy problems," *American Economic Review*, 2015, *105* (5), 491–495.

Koopmans, Tjalling C, "Measurement without theory," *The Review of Economics and Statistics*, 1947, *29* (3), 161–172.

Kozak, Serhiy, Stefan Nagel, and Shrihari Santosh, "Shrinking the cross-section," *Journal of Financial Economics*, 2020, *135* (2), 271–292.

Krishnamurthy, Arvind and Tyler Muir, "How credit cycles across a financial crisis," *The Journal of Finance*, 2025, *80* (3), 1339–1378.

Kyle, Albert S, "Continuous Auctions and Insider Trading," *Econometrica*, 1985, *53* (6), 1315–1335.

Laffont, Jean-Jacques and Jean Tirole, "Using Cost Observation to Regulate Firms," *Journal of Political Economy*, 1986, *94* (3), 614–641.

Lei, Jing, Max G'Sell, Alessandro Rinaldo, Ryan J Tibshirani, and Larry Wasserman, "Distribution-Free Predictive Inference for Regression," *Journal of the American Statistical Association*, 2018, *113* (523), 1094–1111.

Leitner, Yaron and Basil Williams, "Model secrecy and stress tests," *The Journal of Finance*, 2023, *78* (2), 1055–1095.

Lorenzoni, Guido, "Inefficient Credit Booms," *The Review of Economic Studies*, 07 2008, *75* (3), 809–833.

Loshchilov, Ilya and Frank Hutter, "Decoupled weight decay regularization," *arXiv preprint arXiv:1711.05101*, 2018.

Lucas, Robert E, "Econometric policy evaluation: A critique," in "Carnegie-Rochester conference series on public policy," Vol. 1 North-Holland 1976, pp. 19–46.

Ma, Yiming, Kairong Xiao, and Yao Zeng, "Mutual fund liquidity transformation and reverse flight to liquidity," *The Review of Financial Studies*, 2022, *35* (10), 4674–4711.

McKay, Alisdair and Christian K Wolf, "What can time-series regressions tell us about policy counterfactuals?," *Econometrica*, 2023, *91* (5), 1695–1725.

Mullainathan, Sendhil and Jann Spiess, "Machine learning: an applied econometric approach," *Journal of Economic Perspectives*, 2017, *31* (2), 87–106.

Nagel, Stefan, *Machine learning in asset pricing*, Princeton University Press, 2021.

Nakamura, Emi and Jón Steinsson, "Identification in macroeconomics," *Journal of Economic Perspectives*, 2018, *32* (3), 59–86.

Orlov, Dmitry, Pavel Zryumov, and Andrzej Skrzypacz, "The design of macroprudential stress tests," *The Review of Financial Studies*, 2023, *36* (11), 4460–4501.

Parlatore, Cecilia and Thomas Philippon, "Designing stress scenarios," *The Journal of Finance*, 2025, *80* (2), 833–873.

Sarkar, Suproteem K, "Economic representations," 2025.

Scarselli, Franco, Marco Gori, Ah Chung Tsoi, Markus Hagenbuchner, and Gabriele Monfardini, "The graph neural network model," *IEEE transactions on neural networks*, 2008, *20* (1), 61–80.

Schularick, Moritz and Alan M Taylor, "Credit booms gone bust: monetary policy, leverage cycles, and financial crises, 1870–2008," *American Economic Review*, 2012, *102* (2), 1029–1061.

Shapiro, Joel and David Skeie, "Information management in banking crises," *The Review of Financial Studies*, 2015, *28* (8), 2322–2363.

Stein, Jeremy C., "Monetary Policy as Financial Stability Regulation*," *The Quarterly Journal of Economics*, 01 2012, *127* (1), 57–95.

Tibshirani, Ryan J., Rina Foygel Barber, Emmanuel J. Candès, and Aaditya Ramdas, "Conformal Prediction Under Covariate Shift," *Advances in Neural Information Processing Systems*, 2019, *32.*

Uhlig, Harald, "A model of a systemic bank run," *Journal of Monetary Economics*, 2010, *57* (1), 78–96.

Vaswani, Ashish, Noam Shazeer, Niki Parmar, Jakob Uszkoreit, Llion Jones, Aidan N Gomez, Łukasz Kaiser, and Illia Polosukhin, "Attention is all you need," *Advances in neural information processing systems*, 2017, *30.*

Vovk, Vladimir, Alexander Gammerman, and Glenn Shafer, *Algorithmic Learning in a Random World*, Springer, 2005.

Williamson, Oliver E, "Corporate finance and corporate governance," *The journal of finance*, 1988, *43* (3), 567–591.

Wu, Zonghan, Shirui Pan, Fengwen Chen, Guodong Long, Chengqi Zhang, and Philip S Yu, "A comprehensive survey on graph neural networks," *IEEE transactions on neural networks and learning systems*, 2020, *32* (1), 4–24.

Xu, Keyulu, Weihua Hu, Jure Leskovec, and Stefanie Jegelka, "How powerful are graph neural networks?," *arXiv preprint arXiv:1810.00826*, 2018.

Online Appendix for
"The Optimal Use of AI in Financial Regulation"

Christopher Clayton Antonio Coppola

May 2026

A Proofs of Propositions in Main Text

A.1 Proof of Lemma 1

Intermediary i's Lagrangian over ℓ_i is

$$\mathcal{L}_i = q_i^T(R_i - p_i) - \ell_i^T(R_i + \tau_i - \gamma) - \frac{1}{2}q_i^T H_i^q q_i - \frac{1}{2}\ell_i^T H_i^\ell \ell_i - \lambda_i^T(A_i^\ell \ell_i - A_i^q q_i - \rho_i),$$

yielding FOCs

$$0 = -(R_i + \tau_i - \gamma) - H_i^\ell \ell_i - A_i^{\ell T}\lambda_i,$$

$$\ell_i = -H_i^{\ell-1}(R_i + \tau_i - \gamma) - H_i^{\ell-1}A_i^{\ell T}\lambda_i.$$

Assuming the rollover constraint binds,

$$A_i^\ell\Big[- H_i^{\ell-1}(R_i + \tau_i - \gamma) - H_i^{\ell-1}A_i^{\ell T}\lambda_i\Big] = A_i^q q_i + \rho_i,$$

$$-\lambda_i = (A_i^\ell H_i^{\ell-1}A_i^{\ell T})^{-1}A_i^\ell H_i^{\ell-1}(R_i + \tau_i - \gamma) + (A_i^\ell H_i^{\ell-1}A_i^{\ell T})^{-1}A_i^q q_i + (A_i^\ell H_i^{\ell-1}A_i^{\ell T})^{-1}\rho_i,$$

and so we have

$$\begin{aligned}\ell_i = {} & H_i^{\ell-1}A_i^{\ell T}(A_i^\ell H_i^{\ell-1}A_i^{\ell T})^{-1}\rho_i + H_i^{\ell-1}A_i^{\ell T}(A_i^\ell H_i^{\ell-1}A_i^{\ell T})^{-1}A_i^q q_i \\ & + \Big[H_i^{\ell-1}A_i^{\ell T}(A_i^\ell H_i^{\ell-1}A_i^{\ell T})^{-1}A_i^\ell H_i^{\ell-1} - H_i^{\ell-1}\Big](R_i + \tau_i - \gamma).\end{aligned}$$

We therefore write

$$\ell_i = \overline{\ell}_i^0 + \Lambda_i^q q_i - \Lambda_i^\tau(\tau_i - \gamma),$$

where

$$\overline{\ell}_i^0 = H_i^{\ell-1}A_i^{\ell T}(A_i^\ell H_i^{\ell-1}A_i^{\ell T})^{-1}\rho_i - \Lambda_i^\tau R_i,$$

$$\Lambda_i^q = H_i^{\ell-1}A_i^{\ell T}(A_i^\ell H_i^{\ell-1}A_i^{\ell T})^{-1}A_i^q,$$

$$\Lambda_i^\tau = H_i^{\ell-1} - H_i^{\ell-1}A_i^{\ell T}(A_i^\ell H_i^{\ell-1}A_i^{\ell T})^{-1}A_i^\ell H_i^{\ell-1}.$$

Arbitrageur maximization yields

$$\gamma = \overline{\gamma} - \Gamma L,$$

$$\gamma = \overline{\gamma} - \Gamma \sum_i \overline{\ell}_i^0 - \Gamma \sum_i \Lambda_i^q q_i + \Gamma \sum_i \Lambda_i^\tau (\tau_i - \gamma),$$

$$\gamma = \left(\mathbb{I} + \Gamma \sum_i \Lambda_i^\tau\right)^{-1} \left(\overline{\gamma} - \Gamma \sum_i \overline{\ell}_i^0\right) - \sum_i \left[\left(\mathbb{I} + \Gamma \sum_i \Lambda_i^\tau\right)^{-1} \Gamma \Lambda_i^q q_i - \left(\mathbb{I} + \Gamma \sum_i \Lambda_i^\tau\right)^{-1} \Gamma \Lambda_i^\tau \tau_i\right],$$

$$\gamma = \overline{\gamma}^e - \Gamma^e \sum_i \left[\Lambda_i^q q_i^* - \Lambda_i^\tau \tau_i^*\right],$$

where we have defined $\overline{\gamma}^e = \left(\mathbb{I} + \Gamma \sum_i \Lambda_i^\tau\right)^{-1} \left(\overline{\gamma} - \Gamma \sum_i \overline{\ell}_i^0\right)$ and $\Gamma^e = \left(\mathbb{I} + \Gamma \sum_i \Lambda_i^\tau\right)^{-1} \Gamma$. Finally substituting back in,

$$\ell_i = \overline{\ell}_i + \Lambda_i^q q_i - \Lambda_i^\tau \tau_i - \sum_i \left[\Lambda_i^{q,e} q_i^* - \Lambda_i^{\tau,e} \tau_i^*\right],$$

where $\overline{\ell}_i = \overline{\ell}_i^0 + \Lambda_i^\tau \overline{\gamma}^e$, $\Lambda_i^{q,e} = \Lambda_i^\tau \Gamma^e \Lambda_i^q$, and $\Lambda_i^{\tau,e} = \Lambda_i^\tau \Gamma^e \Lambda_i^\tau$.

A.2 Proof of Proposition 1

From Lemma 1, equilibrium liquidations given (q, τ) are

$$\ell_i = \overline{\ell}_i + \Lambda_i^q q_i - \Lambda_i^\tau \tau_i - \sum_i \left[\Lambda_i^{q,e} q_i - \Lambda_i^{\tau,e} \tau_i\right].$$

We define $\overline{\Lambda}_i^\tau = (e_i \otimes I_N)^T \Lambda_i^\tau - (\Lambda_1^{\tau,e}, \ldots, \Lambda_I^{\tau,e})$ (where e_i is the standard basis vector whose i^{th} element is 1 and $\otimes$ is the Kronecker product) and similarly define $\overline{\Lambda}_i^q = (e_i \otimes I_N)^T \Lambda_i^q q_i - (\Lambda_1^{q,e}, \ldots, \Lambda_I^{q,e})$. We then write

$$\ell_i = \overline{\ell}_i + \overline{\Lambda}_i^q q - \overline{\Lambda}_i^\tau \tau.$$

Stacking over i, we have

$$\ell = \overline{\ell} + \overline{\Lambda}^q q - \overline{\Lambda}^\tau \tau.$$

Next, we can write the regulator's objective as

$$\mathbb{E}\left[\sum U_i - \delta(\tau) \middle| s, M\right] = \mathbb{E}\left[\sum_i \mathcal{L}_i \middle| s, M\right] + \mathbb{E}\left[\tau^T \ell \middle| s, M\right] - \frac{1}{2} \tau^T \Delta \tau,$$

where as in the proof of Lemma 1 we have defined the intermediary i Lagrangian by

$$\mathcal{L}_i = q_i^T (R_i - p_i) - \ell_i^T (R_i + \tau_i - \gamma) - \frac{1}{2} q_i^T H_i^q q_i - \frac{1}{2} \ell_i^T H_i^\ell \ell_i - \lambda_i^T (A_i^\ell \ell_i - A_i^q q_i - \rho_i).$$

The regulator thus solves

$$\max_\tau \mathbb{E}\left[\sum_i \mathcal{L}_i \middle| s, M\right] + \mathbb{E}\left[\tau^T \ell \middle| s, M\right] - \frac{1}{2} \tau^T \Delta \tau$$

subject to

$$\ell = \overline{\ell} + \overline{\Lambda}^q q - \overline{\Lambda}^\tau \tau,$$

$$\gamma = \overline{\gamma} - \Gamma L.$$

By the Envelope Theorem, we have the regulator's FOC given by

$$0 = \mathbb{E}\Big[-\ell + \sum_i \ell_i \frac{\partial \gamma}{\partial \tau}\Big| s, M\Big] + \mathbb{E}\Big[\frac{\partial \tau^T \ell}{\partial \tau}\Big| s, M\Big] - \Delta\tau,$$

$$0 = \mathbb{E}\Big[\sum_i (\overline{\Lambda}_i^\tau)^T \Gamma^T L \Big| s, M\Big] + \mathbb{E}\Big[-\overline{\Lambda}^{\tau T}\tau \Big| s, M\Big] - \Delta\tau.$$

Writing $L = L(q) - \sum_i (\overline{\Lambda}_i^\tau)\tau$ and using the assumption that Γ is symmetric,

$$\mathbb{E}[\overline{\Lambda}^{\tau T}|s, M] + \Delta\tau = \mathbb{E}\Big[\sum_i (\overline{\Lambda}_i^\tau)^T \Gamma \Big(L(q) - \sum_i (\overline{\Lambda}_i^\tau)\tau \Big) \Big| s, M\Big],$$

$$\tau = \mathbb{E}\Big[\Xi \Big| s, M\Big]^{-1} \mathbb{E}\Big[(\sum_i \overline{\Lambda}_i^\tau)^T \Gamma L(q) \Big| s, M\Big],$$

where $\Xi = \overline{\Lambda}^{\tau T} + (\sum_i \overline{\Lambda}_i^\tau)^T \Gamma^T (\sum_i \overline{\Lambda}_i^\tau) + \Delta$.

A.3 Proof of Proposition 2

We begin with an intermediate Lemma characterizing the regulator's welfare function. As a preliminary to the Lemma, we define $\theta_i(q) = R_i - (\overline{\gamma} - \Gamma L(q))$ to be the fire sale losses to intermediary i from selling assets prior to maturity in the event of no regulatory intervention. We define $\hat{L}(q) = \mathbb{E}[L(q)|s, M]$ to be predicted total liquidations, given a model M and signal s.

Lemma 2. *Under predictive-causal independence, the regulator's ex-ante expected welfare given positions q and a model M is*

$$\begin{aligned} V(q, M) =& \mathbb{E}_0\Big[q^T(R - p) - \ell(q)^T \theta(q) - \frac{1}{2} q^T H^q q - \frac{1}{2}\ell(q)^T H^\ell \ell(q)\Big] \\ &+ \frac{1}{2} L_0(q)^T \Theta_0 L_0(q) + \frac{1}{2}\mathrm{tr}\Big(\Theta_0\, cov_0(\hat{L}(q))\Big), \end{aligned} \tag{A.1}$$

where $\Theta_0 = \mathbb{E}_0[\Upsilon^T \Psi \Upsilon | M]$, *where* $\Psi = \mathbb{E}\Big[2(\sum_i \overline{\Lambda}_i^\tau)^T \Gamma (\sum_i \overline{\Lambda}_i^\tau) + \Delta + \overline{\Lambda}^{\tau T} H^\ell \overline{\Lambda}^\tau \Big| s, M\Big]$, *and where* $\Upsilon = \Big(\mathbb{E}\Big[\Xi \Big| s, M\Big]\Big)^{-1} \mathbb{E}\Big[(\sum_i \overline{\Lambda}_i^\tau)^T \Gamma \Big| s, M\Big]$.

Using Lemma 2, the welfare gain of a predictive model relative to using just the prior is[1]

$$\Delta V = \frac{1}{2}\operatorname{tr}(\Theta_0 \operatorname{cov}(\widehat{L})).$$

The maximum welfare gain within the class of predictive models is attained by a perfect predictive signal ($\widehat{L} = L$), so:

$$\Delta V_{\max} = \frac{1}{2}\operatorname{tr}(\Theta_0 \operatorname{cov}(L)).$$

Given a weighting matrix W, the W-weighted correlation between the predictions $\widehat{L}$ and the true liquidations L is:

$$\rho_W \equiv \frac{\operatorname{Cov}_W(L, \widehat{L})}{\sqrt{\operatorname{Var}_S(L)\operatorname{Var}_W(\widehat{L})}}.$$

For W deterministic and since $\mathbb{E}L = \mathbb{E}\widehat{L}$ by the law of iterated expectations, we have that:

$$\operatorname{Cov}_W(L, \widehat{L}) := \mathbb{E}\left[(L - \mathbb{E}L)^T W(\widehat{L} - \mathbb{E}L)\right] = \mathbb{E}\left[(\mathbb{E}[L \mid s] - \mathbb{E}L)^T W(\mathbb{E}[L \mid s] - \mathbb{E}L)\right] = \operatorname{Var}_W(\widehat{L}).$$

Therefore:

$$\rho_W^2 = \frac{\operatorname{Var}_W(\widehat{L})^2}{\operatorname{Var}_W(\widehat{L})\operatorname{Var}_W(L)} = \frac{\operatorname{Var}_W(\widehat{L})}{\operatorname{Var}_W(L)}.$$

Using the fact that $\operatorname{Var}_W(X) = \mathbb{E}\left[(X - \mathbb{E}[X])^T W(X - \mathbb{E}[X])\right] = \operatorname{tr}(W \operatorname{cov}(X))$, we then have that:

$$\rho_W^2 = \frac{\operatorname{tr}(W \operatorname{cov}(\widehat{L}))}{\operatorname{tr}(W \operatorname{cov}(L))}.$$

Therefore, $\Delta V = \Delta V_{\max} \cdot \rho^2_{\Theta_0}$.

A.3.1 Proof of Lemma 2

As in the proof of Proposition 1, the regulator's ex-ante expected welfare given positions q, a model M, and a signal s is

$$V(q, M, s) = \mathbb{E}\left[q^T(R - p) - \frac{1}{2}q^T H^q q \middle| s, M\right] + \mathbb{E}\left[\sum_i \left[-\ell_i^T(R_i - \gamma) - \frac{1}{2}\ell_i^T H_i^\ell \ell_i\right] - \frac{1}{2}\tau^T \Delta\tau \middle| s, M\right],$$

where we define H^q to be the block diagonal matrix whose diagonal elements are H_i^q. We define $\theta_i(q) = R_i - \overline{\gamma} + \Gamma L(q)$ to obtain:

$$V(q, M, s) = \mathbb{E}\left[q^T(R - p) - \frac{1}{2}q^T H^q q \middle| s, M\right] + \mathbb{E}\left[-\ell^T\theta(q) + L^T\Gamma\sum_i(\overline{\Lambda}_i^\tau)\tau - \frac{1}{2}\ell_i^T H_i^\ell \ell_i - \frac{1}{2}\tau^T\Delta\tau \middle| s, M\right],$$

[1] For a predictive model, Θ_0 is invariant to the model M. If the regulator only uses the prior, then $cov_0(\hat{L}(q)) = 0$ since $\hat{L}(q) = L_0(q)$.

$$V(q,M,s) = \mathbb{E}\Bigg[q^T(R-p) - \frac{1}{2}q^T H^q q - \ell(q)^T\theta(q)\Bigg|s,M\Bigg] + \mathbb{E}\Bigg[\tau^T\overline{\Lambda}^{\tau T}\theta(q) + \tau^T(\sum_i \overline{\Lambda}_i^\tau)^T\Gamma\Bigg(L(q) - (\sum_i \overline{\Lambda}_i^\tau)\tau\Bigg) - \frac{1}{2}\ell_i^T H_i^\ell \ell_i - \frac{1}{2}\tau^T\Delta\tau\Bigg|s,M\Bigg],$$

$$V(q,M,s) = \mathbb{E}\Bigg[q^T(R-p) - \frac{1}{2}q^T H^q q - \ell(q)^T\theta(q)\Bigg|s,M\Bigg] + \mathbb{E}\Bigg[\tau^T\Bigg(\overline{\Lambda}^{\tau T}\theta(q) + (\sum_i \overline{\Lambda}_i^\tau)^T\Gamma L(q)\Bigg) - \tau^T\Bigg((\sum_i \overline{\Lambda}_i^\tau)^T\Gamma(\sum_i \overline{\Lambda}_i^\tau) + \frac{1}{2}\Delta\Bigg)\tau - \frac{1}{2}\ell^T H^\ell \ell\Bigg|s,M\Bigg].$$

From here, we can expand out

$$\ell^T H^\ell \ell = \Bigg(\ell(q)^T - \tau^T\overline{\Lambda}^{\tau T}\Bigg)H^\ell\Bigg(\ell(q) - \overline{\Lambda}^\tau\tau\Bigg) = \ell(q)^T H^\ell \ell(q) - 2\tau^T\overline{\Lambda}^{\tau T}H^\ell\ell(q) + \tau^T\overline{\Lambda}^{\tau T}H^\ell\overline{\Lambda}^\tau\tau,$$

and substitute back in to obtain

$$\begin{aligned}V(q,M,s) = \mathbb{E}\Bigg[q^T(R-p) - \frac{1}{2}q^T H^q q - \ell(q)^T\theta(q) - \frac{1}{2}\ell(q)^T H^\ell\ell(q)\Bigg|s,M\Bigg] \\ + \mathbb{E}\Bigg[\tau^T\Bigg(\overline{\Lambda}^{\tau T}\theta(q) + (\sum_i \overline{\Lambda}_i^\tau)^T\Gamma L(q) + \overline{\Lambda}^{\tau T}H^\ell\ell(q)\Bigg) \\ - \frac{1}{2}\tau^T\Bigg(2(\sum_i \overline{\Lambda}_i^\tau)^T\Gamma(\sum_i \overline{\Lambda}_i^\tau) + \Delta + \overline{\Lambda}^{\tau T}H^\ell\overline{\Lambda}^\tau\Bigg)\tau\Bigg|s,M\Bigg].\end{aligned}$$

Note that this welfare function is necessarily equivalent to that obtained in Proposition 1. Therefore, an optimal tax formula that is equivalent to that in Proposition 1 yields:

$$\tau = \mathbb{E}\Bigg[2(\sum_i \overline{\Lambda}_i^\tau)^T\Gamma(\sum_i \overline{\Lambda}_i^\tau) + \Delta + \overline{\Lambda}^{\tau T}H^\ell\overline{\Lambda}^\tau\Bigg|s,M\Bigg]^{-1}\mathbb{E}\Bigg[\overline{\Lambda}^{\tau T}\theta(q) + (\sum_i \overline{\Lambda}_i^\tau)^T\Gamma L(q) + \overline{\Lambda}^{\tau T}H^\ell\ell(q)\Bigg|s,M\Bigg].$$

Accordingly substituting back into welfare, we have

$$\begin{aligned}V(q,M,s) =& \mathbb{E}\Bigg[q^T(R-p) - \frac{1}{2}q^T H^q q - \ell(q)^T\theta(q) - \frac{1}{2}\ell(q)^T H^\ell\ell(q)\Bigg|s,M\Bigg] \\ &+ \frac{1}{2}\tau^T\mathbb{E}\Bigg[2(\sum_i \overline{\Lambda}_i^\tau)^T\Gamma(\sum_i \overline{\Lambda}_i^\tau) + \Delta + \overline{\Lambda}^{\tau T}H^\ell\overline{\Lambda}^\tau\Bigg|s,M\Bigg]\tau.\end{aligned}$$

We can then characterize the expected welfare gains by

$$\begin{aligned}V(q,M) =& \mathbb{E}_0\Bigg[q^T(R-p) - \frac{1}{2}q^T H^q q - \ell(q)^T\theta(q) - \frac{1}{2}\ell(q)^T H^\ell\ell(q)\Bigg|M\Bigg] \\ &+ \frac{1}{2}\mathbb{E}_0\Bigg[\tau^T\mathbb{E}\Bigg[2(\sum_i \overline{\Lambda}_i^\tau)^T\Gamma(\sum_i \overline{\Lambda}_i^\tau) + \Delta + \overline{\Lambda}^{\tau T}H^\ell\overline{\Lambda}^\tau\Bigg|s,M\Bigg]\tau\Bigg|M\Bigg],\end{aligned}$$

where τ is given as in Proposition 1.

From here, we define $\Psi = \mathbb{E}\left[2(\sum_i \overline{\Lambda}_i^\tau)^T\Gamma(\sum_i \overline{\Lambda}_i^\tau)+\Delta+\overline{\Lambda}^{\tau T}H^\ell\overline{\Lambda}^\tau\middle| s, M\right]$, and note that $\Psi^T = \Psi$. We can then write more compactly,

$$\begin{aligned}V(q, M) =&\mathbb{E}_0\left[q^T(R-p) - \frac{1}{2}q^T H^q q - \ell(q)^T\theta(q) - \frac{1}{2}\ell(q)^T H^\ell \ell(q)\middle| M\right]\\ &+ \frac{1}{2}\mathbb{E}_0\left[\tau^T\Psi\tau\middle| M\right].\end{aligned}$$

Predictive-Causal Independence. Under predictive-causal independence, we have

$$\tau^* = \mathbb{E}\left[\Xi\middle| s, M\right]^{-1}\mathbb{E}\left[(\sum_i \overline{\Lambda}_i^\tau)^T\Gamma\middle| s, M\right]\mathbb{E}\left[L(q)\middle| s, M\right].$$

We therefore define $\Upsilon = \mathbb{E}\left[\Xi\middle| s, M\right]^{-1}\mathbb{E}\left[(\sum_i \overline{\Lambda}_i^\tau)^T\Gamma\middle| s, M\right]$ and define $\Theta = \Upsilon^T\Psi\Upsilon$. Then, defining $\hat{L}(q) = \mathbb{E}[L(q)|s, M]$ to be predicted liquidations, we have:

$$\begin{aligned}V(q, M) =&\mathbb{E}_0\left[q^T(R-p) - \frac{1}{2}q^T H^q q - \ell(q)^T\theta(q) - \frac{1}{2}\ell(q)^T H^\ell \ell(q)\middle| M\right]\\ &+ \frac{1}{2}\mathbb{E}_0\left[\hat{L}(q)^T\Theta\hat{L}(q)\middle| M\right].\end{aligned}$$

Using predictive-causal independence, we have:

$$\begin{aligned}V(q, M) =& \mathbb{E}_0\left[q^T(R-p) - \frac{1}{2}q^T H^q q - \ell(q)^T\theta(q) - \frac{1}{2}\ell(q)^T H^\ell \ell(q)\middle| M\right]\\ &+ \frac{1}{2}\mathbb{E}_0\left[\hat{L}(q)^T\Theta_0\hat{L}(q)\middle| M\right].\end{aligned}$$

Finally, expanding the second line, we obtain

$$\begin{aligned}V(q, M) =&\mathbb{E}_0\left[q^T(R-p) - \frac{1}{2}q^T H^q q - \ell(q)^T\theta(q) - \frac{1}{2}\ell(q)^T H^\ell \ell(q)\middle| M\right]\\ &+ \frac{1}{2}L_0(q)^T\Theta_0 L(q) + \frac{1}{2}\mathrm{tr}(\Theta_0 cov_0(\hat{L}(q))).\end{aligned}$$

B Architecture and Training Details

This appendix provides the detailed specifications deferred from Section 2.

Multi-Head Attention Computation. We allow for S_A distinct and independent attention heads. For each head $s \in \{1, \ldots, S_A\}$, we compute query, key, and value projections using learnable

projection matrices $W_q^{(\ell,s)}, W_k^{(\ell,s)} \in \mathbb{R}^{d_k \times d_h}$ and $W_v^{(\ell,s)} \in \mathbb{R}^{d_v \times d_h}$, where $d_k = d_v = d_h/S_A$. Define

$$Q_{v,t}^{(\ell,s)} = W_q^{(\ell,s)} h_{v,t}^{(\ell-1)}, \qquad K_{u,t}^{(\ell,s)} = W_k^{(\ell,s)} h_{u,t}^{(\ell-1)}, \qquad V_{u,t}^{(\ell,s)} = W_v^{(\ell,s)} M_{u,t}^{(\ell)}. \tag{A.2}$$

For each edge (v, u), attention weights are formed by a neighborhood softmax, incorporating the normalized edge exposure $\tilde{w}_{vu,t}$ as an additive log-bias:

$$\alpha_{vu,t}^{(\ell,s)} = \frac{\exp\left(\frac{(Q_{v,t}^{(\ell,s)})^T K_{u,t}^{(\ell,s)}}{\sqrt{d_k}} + \log \tilde{w}_{vu,t} \right)}{\sum_{u' \in \mathcal{N}_t(v)} \exp\left(\frac{(Q_{v,t}^{(\ell,s)})^T K_{u',t}^{(\ell,s)}}{\sqrt{d_k}} + \log \tilde{w}_{vu',t} \right)}. \tag{A.3}$$

This ensures $\sum_{u \in \mathcal{N}_t(v)} \alpha_{vu,t}^{(\ell,s)} = 1$ for each head and node. The aggregated message for each node is

$$m_{v,t}^{(\ell,s)} = \sum_{u \in \mathcal{N}_t(v)} \alpha_{vu,t}^{(\ell,s)} V_{u,t}^{(\ell,s)}, \qquad m_{v,t}^{(\ell)} = \frac{1}{S_A} \sum_{s=1}^{S_A} m_{v,t}^{(\ell,s)}. \tag{A.4}$$

Loss Functions. For the masked autoencoder (MAE) objective, masked position sizes are predicted as $\hat{w}_{ia,t} = f_{\text{AE}}(e_{i,t}, e_{a,t})$. The autoencoder loss is $\mathcal{L}_{\text{AE}} = \sum_{(i,a) \in \mathcal{V}_{\text{masked},t}} (g(w_{ia,t}) - g(\hat{w}_{ia,t}))^2$, where $g(\cdot) = \text{sgn}(\cdot) \log(|\cdot|)$. The supervised trade prediction loss combines binary cross-entropy for the extensive margin and mean squared error for the intensive margin:

$$\mathcal{L}_{\text{TP}} = \sum_{(i,a) \in \mathcal{V}_t} \text{BCE}(\hat{c}_{ia,t+1}, \mathbf{1}[y_{ia,t+1} \neq 0]) + \sum_{\substack{(i,a) \in \mathcal{V}_t \\ y_{ia,t+1} \neq 0}} (y_{ia,t+1} - \hat{m}_{ia,t+1})^2, \tag{A.5}$$

where $\text{BCE}(\hat{c}, y) = -[y \log \sigma(\hat{c}) + (1 - y) \log(1 - \sigma(\hat{c}))]$. The overall training procedure minimizes these losses sequentially:

$$\text{Phase 1: } \min_{\Theta_{\text{Backbone}}, \Theta_{\text{AE}}} \mathcal{L}_{\text{AE}}, \qquad \text{Phase 2: } \min_{\Theta_{\text{Backbone}}, \Theta_{\text{TP}}} \mathcal{L}_{\text{TP}}, \tag{A.6}$$

where Θ_{Backbone}, Θ_{AE}, and Θ_{TP} denote the learnable parameter vectors for the GNN backbone, masked autoencoder head, and trade prediction head, respectively.

Model Parameters. The trainable components include the feature map ϕ, the pre-embedding functions for categorical characteristics, the message feed-forward layers $M^{(\ell)}$, the attention mechanism projection matrices W_{qs} and W_{ks}, the node update function $U^{(\ell)}$, the embeddings projection layer ρ, and the task-specific prediction heads f_{AE} and f_{TP}. We collect the set of parameters in all these learnable components in the vector Θ.[2]

[2] All feed-forward layers in our architecture use GELU non-linearities (Hendrycks and Gimpel 2016). These help avoid dead gradients during training.

Table A.I: **Informational content of learned embeddings**

Measure	Value
All obs. $\rightarrow$ investor embeddings (R^2)	0.535
All obs. $\rightarrow$ asset embeddings (R^2)	0.495
Asset embeddings sim. $\leftrightarrow$ co-holding (ρ, all)	0.267
Asset embeddings sim. $\leftrightarrow$ co-holding (ρ, same class)	0.269
Asset embeddings sim. $\leftrightarrow$ co-holding (ρ, different class)	0.234

Notes: The table reports the variance-weighted R^2 of all observable characteristics jointly predicting each embedding dimension, and Pearson correlations between pairwise asset embedding cosine similarity and log co-holding (number of shared investors) for asset pairs with at least one shared holder.

C A Back-of-the-Envelope Welfare Calibration

We provide a rough back-of-the-envelope calibration of the welfare implications of the model's predictions. This exercise rests on several simplifying approximations and is intended to give a sense of magnitudes rather than precise welfare estimates. Proposition 2 shows that the welfare gain from a predictive model is

$$\Delta V(M) = \Delta V_{\max} \cdot \rho^2_{\Theta_0}(M), \tag{A.7}$$

where $\Delta V_{\max} = \frac{1}{2}\text{tr}(\Theta_0 \,\text{cov}(L))$ is the welfare gain from a perfect forecast and $\rho^2_{\Theta_0}(M)$ is the model's Θ_0-weighted R-squared. We calibrate each component in turn.

We approximate Θ_0 using Harberger deadweight losses from fire-sale price distortions. The welfare weight for asset a is calibrated to be:

$$\theta_a = \frac{v_a}{\text{ADV}_a^{2\beta}}, \tag{A.8}$$

where $v_a = \sum_i w_{ia}$ is total held value, ADV_a is average daily dollar volume, and $\beta = 0.25$ is the permanent price impact exponent.[3] This parameterization isolates the price-impact component of Θ_0. In the full model (Proposition 2), Θ_0 also reflects the regulatory cost Δ and the holding cost channel through H^ℓ; to the extent that these additional channels are quantitatively important, our calibration understates the welfare weight on assets with high adjustment costs. Using this calibration, and taking the out-of-sample predictive performance of the GNN model on the cross-sectional trade prediction task as a proxy for the predictive performance on the theoretical targeting statistics, we obtain a Θ_0-weighted R-squared value of $\rho^2_{\Theta_0} = 10.8\%$.

The most challenging object to calibrate is $\Delta V_{\max}$, the welfare gain from perfectly targeted

[3] Kyle (1985) derives $\lambda \propto 1/\sqrt{V}$ ($\beta = 0.5$) for temporary impact. The permanent component decays more slowly: $\beta \approx 0.2$–0.4 in the literature (Bouchaud et al., 2018).

Table A.II: **Calibrated welfare gains from predictive models**

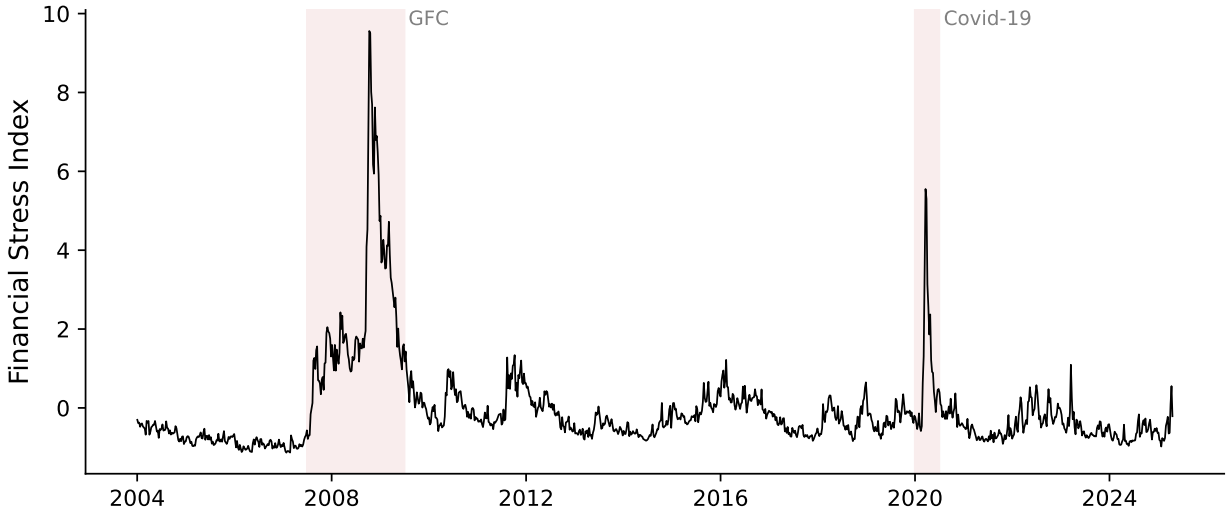
	Fire-sale externality $\Delta V_{\max}$ (% of consumption)					
	0.5%		2.0%		5.0%	
Model ($\rho^2_{\Theta_0}$)	\$B	% C	\$B	% C	\$B	% C
Ridge regression (1.6%)	\$0.9B	0.008%	\$3.7B	0.032%	\$9.2B	0.08%
Graph transformer (10.8%)	\$6.2B	0.054%	\$24.8B	0.22%	\$62.1B	0.54%

Notes: Welfare calibration using Proposition 2: $\Delta V(M) = \Delta V_{\max} \cdot \rho^2(M)$. Each column uses a different calibration of $\Delta V_{\max}$ as a fraction of aggregate consumption ($C = \$11.5$T annual PCE).

intervention. We consider three values spanning the range of estimates in the literature.[4] The lower bound of $\Delta V_{\max} = 0.5\%$ of consumption is the order of magnitude implied by Bianchi (2011) and Elenev et al. (2021), who estimate the welfare costs of overborrowing externalities and the gains from optimal bank capital regulation, respectively. The upper bound of $\Delta V_{\max} = 5\%$ corresponds to higher risk aversion ($\gamma \approx 10$), consistent with the intermediary asset pricing literature and with empirical evidence on the magnitude of investment disruptions caused by fire-sale dynamics (Coppola 2025). The middle value of $\Delta V_{\max} = 2\%$ is a central estimate. Table A.II reports the calibrated welfare gains from deploying the graph transformer versus a ridge regression baseline. The graph transformer delivers welfare gains ranging from \$6.2B ($\Delta V_{\max} = 0.5\%$) to \$62.1B ($\Delta V_{\max} = 5\%$), roughly five times the gains from the best traditional baseline across all calibrations.

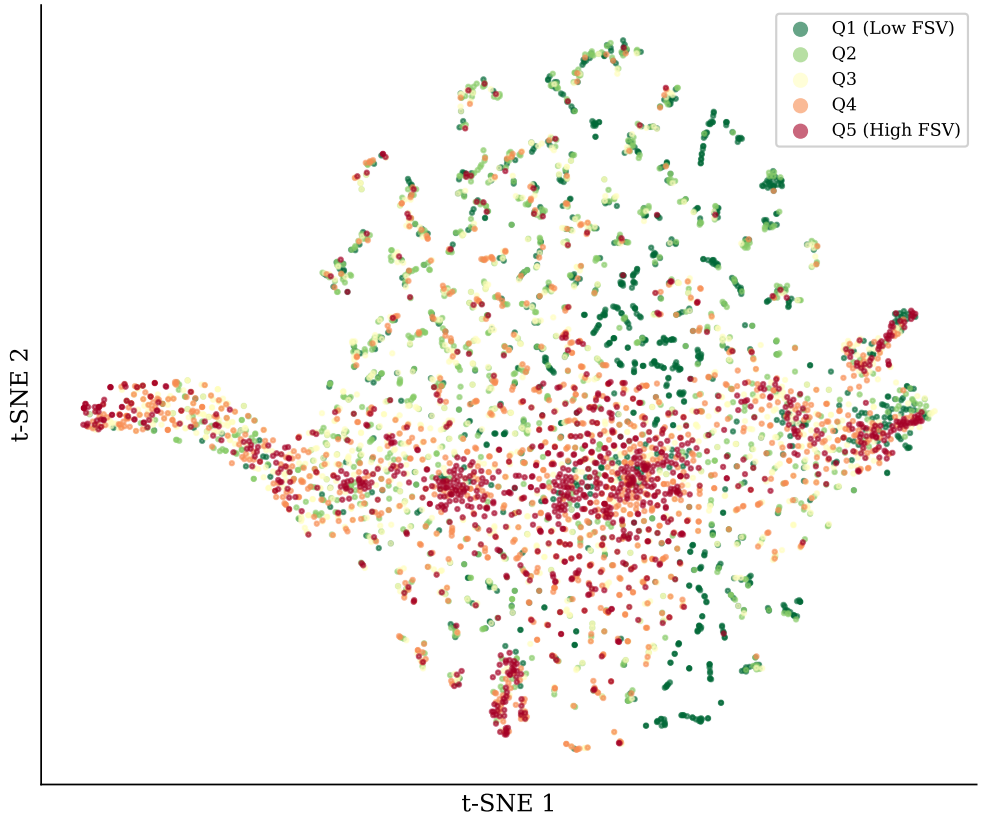
[4] We use mean US personal consumption expenditures as the consumption base, following Bianchi (2011) and Elenev, Landvoigt and Van Nieuwerburgh (2021).

Figure A.I: **St. Louis Fed Financial Stress Index**



Notes: Weekly observations; shaded regions indicate the Global Financial Crisis (2007–2009) and the Covid-19 crisis (2020). The index is centered at zero, with positive values indicating above-average financial stress.

Figure A.II: **Asset embeddings encode fire-sale vulnerability**



Notes: t-SNE projection of asset embeddings from the 2019Q4 cross-section, colored by quintile of the fire-sale vulnerability (FSV) score. FSV is defined as the product of flow-sensitive holder share (fraction held by open-end mutual funds or ETFs) and asset illiquidity (1/ADV). Each point represents an asset's 128-dimensional GNN embedding, projected to two dimensions via t-SNE (perplexity = 50, 2,000 iterations). High-FSV assets (Q5, dark red) cluster in distinct regions of the embedding space, confirming that the GNN's learned representations encode the crowdedness-illiquidity interaction that governs fire-sale externalities.

D Theory Appendix

In this appendix, we extend the setup to incorporate a date 0 in which asset positions are chosen. The structure of dates 1 and 2 are the same as before.

Intermediaries. At date 0, intermediary i invests in a vector $q_i = (q_{i1}, \ldots, q_{iN})^T$ of assets. If $q_{in} < 0$, then intermediary i has undertaken a negative investment (shorting) asset n.[5] The cost to intermediary i of producing the asset vector q_i is $C_i(q_i) = p_i^T q_i - \frac{1}{2} q_i^T H_i^q q_i$, where p_{in} is the per-unit cost to i of producing asset n and where $p_i = (p_{i1}, \ldots, p_{iN})^T$. The cost component $q_i^T H_i^q q_i$ is a quadratic adjustment/holding cost, where H_i^q is an $N \times N$ matrix. Intermediary i's total payoff (consumption) at date 2, including costs incurred at date 0, is

$$U_i = q_i^T (R_i - p_i) - \ell_i^T (R_i - \gamma) - \frac{1}{2} q_i^T H_i^q q_i - \frac{1}{2} \ell_i^T H_i^\ell \ell_i. \tag{A.9}$$

Information Structure at Date 0. We assume that although nature draws the true parameters at date 0, all agents at date 0 are uncertain about the true values of the parameters $\Phi = \{A_i^q, A_i^\ell, H_i^\ell, \rho_i, R_i, \overline{\gamma}\}$. All agents, including the regulator, have a common prior $\Phi \sim \mu_0$ at date 0.[6] At date 1, as in the baseline setup, the true model parameters become common knowledge of private agents, and the problem unfolds as in the main text.[7]

Competitive Equilibrium. We define a competitive equilibrium as follows.

Definition 4. *A competitive equilibrium of the model, given true model parameters Φ, is a vector of prices γ and a set of allocations $\{q_i, \ell_i, L\}$ such that:*

1. *At date 1, taking as given asset allocations $\{q_i\}$ and model parameters Φ:*
   - *(a) Intermediary i chooses ℓ_i to maximize utility (equation A.9) subject to the rollover constraint (12), taking prices γ as given.*
   - *(b) Arbitrageurs choose L maximize utility (equation 14), taking prices γ as given.*
   - *(c) The liquidation markets clear (equation 15).*
2. *At date 0:*
   - *(a) Intermediary i chooses q_i to maximize expected utility $\mathbb{E}_0[U_i]$, where $\mathbb{E}_0$ denotes the expectation given the prior μ_0 over model parameters Φ.*

[5] We could endow intermediaries with a stock of assets, but for expositional convenience we set that stock to 0.

[6] In practice, intermediaries may hold more precise priors over model parameters than the regulator, in which case the regulator could also infer structural information from observed portfolio choices. One advantage of the ex-post intervention in such an extension would be its ability to react to information revealed by intermediaries' choices, potentially reducing risks of moral hazard or imperfectly calibrated regulation ex ante.

[7] Assuming that private agents and the regulator have a common prior at date 0 simplifies analysis because it prevents the regulator from learning information about these parameters from inference about private sector beliefs based on the asset allocation. It also eliminates a regulatory incentive based on different beliefs the regulator and agents (e.g., Fontanier 2025.)

D.1 Expected Welfare from a Model and Optimal Model Choice

We next ask how a regulator at date 1 would choose a model $M \in \mathcal{M}$ under discretion, taking as given the asset holdings q of intermediaries. We maintain simplicity by assuming predictive-causal independence for the main text (Definition 2) and by focusing on predictive models (Definition 3).

We assume that the regulator faces a separable utility cost $\mathcal{C}(M, q)$ from adopting (predictive) model $M \in \mathcal{M}$. In Lemma 2, for a predictive model (Definition 3) the key sufficient statistic of the model from a welfare perspective is the prior covariance matrix over the ex-post prediction of liquidations, $\Sigma_0^{\hat{L}} = cov_0(\hat{L}(q))$. The matrix Θ_0 and the averaged expected liquidations $L_0(q)$ are invariant to model choice. For symmetric matrices $\Sigma_0^{\hat{L}}$ that are attainable from some model M, we can therefore re-represent costs as $C(\Sigma_0^{\hat{L}}, q) = \inf_{M \in \mathcal{M} | cov_0(\hat{L}(q)) = \Sigma_0^{\hat{L}}} \mathcal{C}(M, q)$. We assume that C is differentiable in $(\Sigma_0^{\hat{L}}, q)$ over an open ball that contains its optimal value.

As a result, for a predictive model we can write the regulator's optimization problem as

$$\max_{\Sigma_0^{\hat{L}}} \frac{1}{2} \text{tr}\left(\Theta_0 \Sigma_0^{\hat{L}}\right) - C(\Sigma_0^{\hat{L}}, q)$$

subject to the constraint that $\Sigma_0^{\hat{L}}$ is a symmetric matrix. We obtain the following result on the optimal predictive model.

Proposition 3. *The regulator's optimal predictive model satisfies*

$$\frac{\partial C(\Sigma_0^{\hat{L}}, q)}{\partial \Sigma_0^{\hat{L}}} + \left(\frac{\partial C(\Sigma_0^{\hat{L}}, q)}{\partial \Sigma_0^{\hat{L}}}\right)^T = \Theta_0 \tag{A.10}$$

where $\frac{\partial C(\Sigma_0^{\hat{L}}, q)}{\partial \Sigma_0^{\hat{L}}}$ *is a square matrix whose ij-th element is* $\frac{\partial C(\Sigma_0^{\hat{L}}, q)}{\partial (\Sigma_0^{\hat{L}})_{ij}}$.

Proposition 3 yields an intuitive trade-off on optimal predictive model choice in terms of choice of covariance matrix of the policy intervention. The regulator is willing to pay a higher marginal cost to increase precision on dimensions where Θ_0 is larger, that is when the policy has greater impact on aggregate liquidations and prices, when the regulatory cost is higher, or when the impact through holding costs is higher. In this sense, there is a complementarity between predictive power and knowledge of the causal policy impact: the regulator is willing to pay larger costs to acquire precise predictions of aggregate liquidations precisely on dimensions on which the policy impact on liquidations and liquidation prices is anticipated to be largest.[8]

[8] In a dynamic extension where the one-shot model is embedded as a stage game played repeatedly, the regulator would face a trade-off between acquiring predictive information useful for the current crisis and uncovering structural parameters valuable for future interventions. We conjecture that predictive models would be relatively myopically useful, providing substantial information for current intervention but limited updating about the true distribution of underlying parameters. This could face the regulator with an interesting dynamic trade-off between myopically acquiring more predictive information, and trying to uncover the true structural parameters that would also be useful for designing regulation and interventions during the next crisis.

D.2 Privately Optimal Asset Allocations

To examine how model choice and ex-post intervention shape the ex-ante asset allocations of intermediaries, we begin by studying the private optimum of individual intermediaries, and then study socially optimal interventions. Intermediary i at date 0 takes as given the model choice M^* of the regulator and the resulting possible equilibria,[9] and solves

$$\max_{q_i} \mathbb{E}_0\left[q_i^T(R_i - p_i) - \ell_i^T(R_i + \tau_i^* - \gamma) - \frac{1}{2}q_i^T H_i^q q_i - \frac{1}{2}\ell_i^T H_i^\ell \ell_i\right].$$

Intermediary i's asset allocation is therefore affected both through the specific intervention τ_i^* anticipated, and also through the liquidation price (which in turn also affects equilibrium liquidations). Intermediary i knows that equilibrium liquidations are determined as in Lemma 1, but only internalizes the effect of its own q_i on its own liquidations (and not on equilibrium liquidation price or equilibrium liquidations, and not on the optimal model choice or intervention).

The following proposition characterizes intermediaries' privately optimal asset allocations.[10]

Proposition 4. *The privately optimal asset allocation satisfies*

$$\mathbb{E}_0\left[H_i^q q_i^* + \Lambda_i^{qT} H_i^{\ell} \overline{\ell}_i(q^*)\right] = \mathbb{E}_0\left[R_i - p_i - \Lambda_i^{qT}\theta_i(q^*)\right] - \mathbb{E}_0\left[\Lambda_i^{qT}\left(\tau_i^* - \left(H_i^{\ell}\overline{\Lambda_i^{\tau}} + \Gamma(\sum_i \overline{\Lambda_i^{\tau}})\right)\tau^*\right]\right. \tag{A.11}$$

Proposition 4 expresses the optimal portfolio choice in the form of a marginal cost-marginal benefit trade-off. The left hand side captures the marginal cost of increasing holdings of an asset, which includes both the ex-ante and ex-post adjustment costs of holding more and liquidating more of an asset. This term is evaluated at the no-intervention benchmark, that is as-if we had $\tau^* = 0$.

The right hand side captures the marginal benefit, which is decomposed into a marginal benefit absent the ex-post regulatory intervention (the first term) plus the marginal benefit arising from the impact of intervention (the second term). The first term on the RHS is the baseline expected asset return, $R_i - p_i$, net of costs of liquidations. The liquidation costs are the amount liquidations are changed by increasing holdings, Λ_i^{qT}, times the fire sale loss in liquidation, $\theta_i(q^*)$.

The final term on the RHS captures the impacts of model choice and the ex-post intervention. This is the only term in equation A.11 that depends on model choice and intervention. It captures the cost of holding an asset induced through regulation. The expectation of ex-post policy intervention has two impacts. First, a higher wedge τ_{in} on intermediary i increases the cost of liquidating asset n, discouraging the intermediary from holding portfolios that result in it liquidating that asset ex post. There are also equilibrium costs of the vector of wedges τ through the equilibrium price. In contrast, here a higher wedge τ_{in} encourages the intermediary i to hold more of an asset when the asset price rises as a result, which partially offsets the benefit from raising the price. This is

[9] Recall that at date 0, the intermediary does not know the true parameters.

[10] Note that Proposition 4 does not rely on predictive-causal independence or a predictive model.

a standard channel of moral hazard. This moral hazard channel is amplified when the regulator's instruments do not cover all holders of a given asset: unregulated intermediaries capture the benefit of higher liquidation prices without bearing any liquidation wedge, and so their ex-ante incentive to accumulate the asset is undeterred by the prospect of intervention.

It is clear that the ex-post intervention affects the optimal asset allocation: a higher expected tax on asset n ex post directly discourages its purchase ex ante, but a higher liquidation price ex post encourages its purchase ex ante. As a result, even a purely predictive model can impact the asset allocation ex ante. In particular, even though under a purely predictive model (Definition 3) the expectation of τ^* is that same as if the regulator ran no model, there is a covariance induced between the tax itself, τ^*, and the impact on liquidations, Λ_i^q, as long as the predictive model is loading at least some on Bayesian inference on the impact of asset holdings on liquidations Λ_i^q. That is to say, focusing on the direct term $\mathbb{E}_0[\Lambda_i^{qT}\tau_i^*]$, for a purely predictive model we can write

$$\mathbb{E}_0\left[\Lambda_i^{qT}\tau_i^*\right] = \mathbb{E}_0\left[\Lambda_i^{qT}\right]\mathbb{E}_0\left[\tau_i\right] + \text{cov}_0\left(\Lambda_i^{qT}, \mathbb{E}_0[\Xi]^{-1}\mathbb{E}_0\left[(\sum_i \overline{\Lambda}_i^{\tau})^T\Gamma\right]\mathbb{E}[L(q)|s,M]\right),$$

where the second term reflects how the true value of Λ_i^q varies with the prediction of liquidations. In a similar fashion, moral hazard can also be exacerbated if the impact of asset allocations on liquidations Λ_i^q is what a key driver of the predictability of ex post liquidations.

More broadly, both the virtuous deterrence and the moral hazard channels are bounded by the precision of the regulator's model: a less granular model generates smaller covariance between the intervention and the structural loadings, and hence attenuates both the beneficial and the adverse feedback of the ex-post intervention on ex-ante portfolio choice.[11]

D.3 Socially Optimal Asset Allocation

Finally, we study the constrained efficient asset allocation q of the regulator. Formally, we assume that the regulator can impose wedges on asset holdings at date 0, that is a revenue-neutral tax $t_i = (t_{i1}, \ldots, t_{iN})^T$. Because the regulator has a complete set of wedges ex ante, this is equivalent to the regulator directly picking portfolio allocations ex ante.[12] The following proposition characterizes the optimal wedges $t = (t_1^T, \ldots, t_I^T)^T$ when the regulator chooses an optimal predictive model ex post.

[11] This gives rise to a potential time-consistency problem in model choice, since the model choice affects ex-ante allocations. The tension is likely more pronounced when the regulator cannot regulate all intermediaries or all assets ex ante. We leave the implications of commitment versus discretion for optimal model design to future work.

[12] It is straightforward to extend results to incomplete ex-ante instruments, but for brevity we focus on complete instruments.

Proposition 5. *For a predictive model, the social planer's optimal date* 0 *portfolio wedges* t *are*

$$\begin{aligned} t =& \mathbb{E}_0\left[(\sum_j \overline{\Lambda}_j^q)^T \Gamma L(q) - \Lambda^{q,eT} \sum_i \left(\theta_i(q) + H_i^\ell \ell_i(q)\right)\right] \\ &+ \frac{dC(\Sigma_0^{\hat{L}}, q)}{dq} - \mathbb{E}_0\left[(\sum_i \overline{\Lambda}_i^q)^T\right]\Theta_0 \mathbb{E}_0[L(q)] - \mathbb{E}_0\left[\Psi\tau\right] \end{aligned} \tag{A.12}$$

where $\mathbb{E}_0[\Psi\tau]$ *is a stacked vector whose* i^{th} *block is* $\mathbb{E}_0\left[\Lambda_i^{qT}\left(\tau_i - \left(\Gamma(\sum_i \overline{\Lambda}_i^\tau) + H_i^\ell \overline{\Lambda}_i^\tau\right)\tau\right)\right]$.

The optimal ex-ante asset tax formula is intuitive and is decomposed into two lines. The first line captures the uninternalized effects of intermediaries increasing holdings of an asset in absence of regulatory intervention. First, as q changes, total liquidations change across intermediaries, resulting in changes in the liquidation price and hence changes in revenue proceeds from total liquidations $L(q)$. Second, changes in forced liquidations through changes in the equilibrium price result in losses due to the size of the discount $\theta_i(q)$ and due to changes in marginal holding costs $H_i^\ell \ell_i(q)$. In absence of an ex-post intervention, this first line would capture the standard macroprudential regulation of asset positions.[13]

The second line captures the interaction of the ex-ante asset regulation with the ex-post model design and intervention. The first term, dC/dq, reflects how the changing assets held by intermediaries affects the cost of acquiring information through the model ex post. The regulator imposes larger holding taxes on asset positions that make running the model more costly ex post. For example, the regulator might discourage holdings of non-transparent or hard-to-assess assets.

The second term on the second line captures the effect on the expected intervention size (the term $L_0(q)^T \Theta_0 L_0(q)$ in equation A.1). Intuitively, concentrations into a position q increase total liquidations on the margin by $\sum_i \overline{\Lambda}_i^q$, which prompts a larger ex post intervention by the regulator. This increase in ex-post intervention helps to manage the fire sale and so mitigates the impact of the ex-ante increase in asset allocation. This gives a first dimension whereby the ex-post intervention provides a partial substitute for the ex-ante asset tax, and leads the regulator to require potentially smaller interventions ex ante, knowing that fire sales will be managed ex post.

Finally, there are the direct and moral hazard effects on intermediaries, $\mathbb{E}_0[\Psi\tau^*]$, are those in the final term in equation A.11 of Proposition 4. First, the prospect of the ex-post tax on liquidations directly discourages holdings of the asset ex ante when holding more promotes liquidations ex post. Second, there is the moral hazard effect: as the liquidation price rises, intermediaries' perceived cost of liquidations $\theta_i(q)$ falls, and so they become more willing to hold more of an asset even if that forces them to liquidate. It is interesting again to observe that for assets for which the direct effect dominates the indirect price effect, the ex-post tax actually serves as a substitute for ex-ante regulation, leading to a smaller intervention t ex ante.

[13] Since our framework allows negative positions $q_{in} < 0$, we can think of these negative positions as liabilities. As such, it also captures regulation of such liabilities.

D.4 Ex-Post Subsidy-Based Interventions

Our baseline analysis assumes that the regulator directly manages liquidations through a wedge/tax on liquidations. In practice, ex-post interventions can also involve "bailout" interventions that subsidize retaining assets rather than taxing selling them (e.g. lender of last resort, debt guarantees). Suppose that rather than taxing liquidations ℓ_i, the regulator instead applies a subsidy on the amount $q_i - \ell_i$ of the asset that is held to maturity. Formally, the payoff to intermediary i at date 2 is now

$$U_i = U_i + (q_i^T - q_i^{*T})\tau_i - (\ell_i^T - \ell_i^{*T})\tau_i,$$

so that the regulator continues to apply revenue-neutral interventions.[14]

Because the regulator at date 1 takes the asset allocations as given, the regulator's optimization problem over both model choice and the ex-post intervention are formally the same as before. Thus, Lemma 1 and Propositions 1-3 continue to apply. However, the privately optimal asset allocation is affected by the subsidy on asset retention. In particular, in Proposition 4, the expected return on holding asset q_i is raised from R_i to $R_i + \tau_i^*$. Intuitively an ex-post subsidy promotes overinvestment in that asset. This gives rise to a familiar channel of moral hazard.

Relative to the case of a liquidation tax, it is worthwhile to note that the only new term for private intermediaries in their optimization problem is the revenue benefits $q_i^T \mathbb{E}_0[\tau_i^*]$ of their asset position. Therefore, relative to the liquidation tax, the regulator's model choice only affects intermediaries' asset allocation ex ante to the extent it changes the expected size of the intervention, $\mathbb{E}_0[\tau_i^*]$. In particular for a predictive model under predictive-causal independence (Definitions 2 and 3), we know that $\mathbb{E}_0[\tau_i^*]$ does not depend on the model used; instead, it is only the covariance matrix of the intervention (its precision) that depends on the model. It is thus interesting and surprising that purely predictive models that help with prediction but not with causal inference do not exacerbate moral hazard relative to the case of the liquidation tax. In contrast, models that are informative about the causal impact of the policy intervention change expectations of the policy intervention, and are potentially associated with moral hazard. The logic is reminiscent of that of Laffont and Tirole (1986) in the context of regulation of a firm with unobservable effort and uncertain costs.

D.5 Relaxed Information Structure for Policy Invariance

The baseline theory assumes that private agents observe the full state Φ in the Middle. This section shows how the policy invariance result can be relaxed under a substantially weaker condition that regulator-generated public information is informative about the predictive component of the state and not about the transmission component.

We illustrate the relaxation as follows. Suppose that private agents are uncertain over the return

[14] Since individual intermediaries take revenue remissions as given, there is still moral hazard from the subsidy.

R_i, sharing a common prior with the regulator, and that the regulator makes public its model M and signal s before private agents choose liquidations; we denote this regulator-supplied information $d = (M, s)$. Let $B \equiv \sum_i \Lambda_i^\tau$, so that $\Xi \equiv \Lambda_\tau^\top + B^\top \Gamma B + \Delta$, where the matrices Λ_i^τ and Ξ are those defined in Proposition 1. Suppose that:

(i) the transmission objects $\Lambda \equiv \{\Lambda_i^q, \Lambda_i^\tau, \Lambda_i^{q,e}, \Lambda_i^{\tau,e}\}_{i=1}^I$ are observed by private agents in the Middle;

(ii) after observing d, private agents update Bayesianly from the common prior.

Define the posterior-predictive no-intervention liquidation vector

$$\widehat{L}_d(q) \equiv \mathbb{E}[L(q) \mid \Lambda, \Xi, d].$$

Then, the proof of Lemma 1 follows as before, with $\mathbb{E}[R_i|d]$ replacing R_i. As a result, we can write

$$L(q, \tau; d) = \widehat{L}_d(q) - B\tau,$$

where $L(q)$ is liquidations absent intervention. All dependence of equilibrium outcomes on the regulator-generated public signal d enters through the posterior-predictive baseline liquidation vector $\widehat{L}_d(q)$; the slope matrices mapping portfolios and wedges into outcomes are unchanged. Then under predictive-causal independence, the regulator's optimal wedges satisfy

$$\tau^*(d) = \Xi^{-1} B^\top \Gamma \widehat{L}_d(q).$$

D.6 Proofs

D.6.1 Proof of Proposition 3

The optimal model choice solves

$$\max_{\Sigma_0^{\hat{L}}} \frac{1}{2} \text{tr}\left(\Theta_0 \Sigma_0^{\hat{L}}\right) - C(\Sigma_0^{\hat{L}}, q)$$

subject to the restriction that $\Sigma_0^{\hat{L}}$ is symmetric. Taking the first order condition, we have

$$\frac{\partial C(\Sigma_0^{\hat{L}}, q)}{\partial \Sigma_0^{\hat{L}}} + \left(\frac{\partial C(\Sigma_0^{\hat{L}}, q)}{\partial \Sigma_0^{\hat{L}}}\right)^T = \Theta_0$$

since Θ_0 is symmetric.

D.6.2 Proof of Proposition 4

The intermediary i ex ante optimization problem is

$$\max_{q_i} \mathbb{E}_0\Big[\sum_i \Big[q_i^T(R_i - p_i) - \ell_i^T(R_i + \tau_i^* - \gamma) - \frac{1}{2}q_i^T H_i^q q_i - \frac{1}{2}\ell_i^T H_i^\ell \ell_i\Big],$$

where we have

$$\ell_i = \overline{\ell}_i + \Lambda_i^q q_i - \sum_j \Lambda_j^{q,e} q_j^* - \overline{\Lambda}_i^\tau \tau^*.$$

So, we have the FOC

$$0 = \mathbb{E}_0\Big[R_i - p_i - \Lambda_i^{qT}(R_i + \tau_i^* - \gamma) - H_i^q q_i - \Lambda_i^{qT} H_i^\ell \ell_i\Big].$$

Substituting in for ℓ_i, we have

$$\mathbb{E}_0\Big[H_i^q\Big]q_i = \mathbb{E}_0\Big[R_i - p_i - \Lambda_i^{qT}(R_i + \tau_i^* - \gamma) - \Lambda_i^{qT} H_i^\ell\Big(\overline{\ell}_i + \Lambda_i^q q_i - \sum_j \Lambda_j^{q,e} q_j^* - \overline{\Lambda}_i^\tau \tau^*\Big)\Big],$$

$$\mathbb{E}_0\Big[H_i^q + \Lambda_i^{qT} H_i^\ell \Lambda_i^q\Big]q_i = \mathbb{E}_0\Big[R_i - p_i - \Lambda_i^{qT}(R_i - \gamma) - \Lambda_i^{qT} H_i^\ell\Big(\overline{\ell}_i - \sum_j \Lambda_j^{q,e} q_j^*\Big)\Big] + \mathbb{E}_0\Big[-\Lambda_i^{qT}\tau_i^* + \Lambda_i^{qT} H_i^\ell \overline{\Lambda}_i^\tau \tau^*\Big].$$

We use that $R_i - \gamma = \theta_i(q^*) - \Gamma(\sum_i \overline{\Lambda}_i^\tau)\tau^*$ to obtain

$$\mathbb{E}_0\Big[H_i^q q_i^* + \Lambda_i^{qT} H_i^\ell \overline{\ell}_i(q^*)\Big] = \mathbb{E}_0\Big[R_i - p_i - \Lambda_i^{qT}\theta_i(q^*)\Big] - \mathbb{E}_0\Big[\Lambda_i^{qT}\Big(\tau_i^* - \Big(H_i^\ell \overline{\Lambda}_i^\tau + \Lambda_i^{qT}\Gamma(\sum_i \overline{\Lambda}_i^\tau)\Big)\tau^*\Big].$$

D.6.3 Proof of Proposition 5

We have that:

$$V(q, M) = \mathbb{E}\Big[q^T(R - p) - \frac{1}{2}q^T H^q q - \ell(q)^T\theta(q) - \frac{1}{2}\ell(q)^T H^\ell \ell(q)\Big] + \frac{1}{2}L_0(q)\Theta_0 L_0(q) + \frac{1}{2}\mathrm{tr}(\Theta_0 cov_0(\hat{L}(q)).$$

Recalling that $\ell_i(q) = \overline{\ell}_i + \overline{\Lambda}_i^q q$, $\theta_i(q) = R_i - \overline{\gamma} + \Gamma L(q)$, and $L(q) = \sum_i \overline{\ell}_i + \sum_i \overline{\Lambda}_i^q q$, then we can expand:

$$\sum_i \ell_i(q)^T\theta_i(q) = \sum_i \overline{\ell}_i^T\theta_i(0) + q^T\sum_i \overline{\Lambda}_i^{qT}\theta_i(0) + q^T(\sum_j \overline{\Lambda}_j^q)^T\Gamma L(0) + q^T\sum_i\Big(\overline{\Lambda}_i^{qT}\Big)\Big(\Gamma\sum_j \overline{\Lambda}_j^q\Big)q,$$

$$\ell(q)H^\ell\ell(q) = \sum_i \overline{\ell}_i^T H_i^\ell \overline{\ell}_i + 2q^T\Big(\sum_i \overline{\Lambda}_i^{qT} H_i^\ell \overline{\ell}_i\Big) + q^T\Big(\sum_i \overline{\Lambda}_i^{qT} H_i^\ell \overline{\Lambda}_i^q\Big)q.$$

For a predictive model, Θ_0 is invariant to the model choice M and to q. Therefore by the

Envelope Theorem,

$$0 = \mathbb{E}_0\Bigg[R - p - H^q q - \Bigg[\sum_i \overline{\Lambda}_i^{qT}\theta_i(0) + (\sum_j \overline{\Lambda}_j^q)^T \Gamma L(0) + 2\sum_i \Big(\overline{\Lambda}_i^{qT}\Big)\Big(\Gamma \sum_j \overline{\Lambda}_j^q\Big)q\Bigg] - \Bigg[\Big(\sum_i \overline{\Lambda}_i^{qT} H_i^\ell \overline{\ell}_i\Big) + \Big(\sum_i \overline{\Lambda}_i^{qT} H_i^\ell \overline{\Lambda}_i^q\Big)q\Bigg]\Bigg] - \frac{dC(\Sigma_0^{\hat{L}}, q)}{dq} + \mathbb{E}_0\Bigg[(\sum_i \overline{\Lambda}_i^q)^T\Bigg]\Theta_0 \mathbb{E}_0[L(q)],$$

$$0 = \mathbb{E}_0\Bigg[R - p - H^q q - \Bigg[\sum_i \overline{\Lambda}_i^{qT}\Big(\theta_i(0) + \Big(\Gamma \sum_j \overline{\Lambda}_j^q\Big)q\Big) + (\sum_j \overline{\Lambda}_j^q)^T \Gamma\Big(L(0) + \sum_j \overline{\Lambda}_j^q q\Big)\Bigg] - \Bigg[\Big(\sum_i \overline{\Lambda}_i^{qT} H_i^\ell \overline{\ell}_i\Big) + \Big(\sum_i \overline{\Lambda}_i^{qT} H_i^\ell \overline{\Lambda}_i^q\Big)q\Bigg]\Bigg] - \frac{dC(\Sigma_0^{\hat{L}}, q)}{dq} + \mathbb{E}_0\Bigg[(\sum_i \overline{\Lambda}_i^q)^T\Bigg]\Theta_0 \mathbb{E}_0[L(q)]\,.$$

We have

$$\theta_i(0) + \Gamma\Big(\sum_j \overline{\Lambda}_j^q\Big)q = \theta_i(q),$$

$$L(0) + \Big(\sum_j \overline{\Lambda}_j^q\Big)q = L(q),$$

so we get:

$$\mathbb{E}_0\Big[H^q q\Big] = \mathbb{E}_0\Big[R - p - \sum_i \overline{\Lambda}_i^{qT}\Big(\theta_i(q) + H_i^\ell \ell_i(q)\Big)\Big] - \mathbb{E}_0\Big[(\sum_j \overline{\Lambda}_j^q)^T \Gamma L(q)\Big] - \frac{dC(\Sigma_0^{\hat{L}}, q)}{dq} + \mathbb{E}_0\Bigg[(\sum_i \overline{\Lambda}_i^q)^T\Bigg]\Theta_0 \mathbb{E}_0[L(q)].$$

Recall that we have

$$\ell_i(q) = \overline{\ell}_i + \Lambda_i^q q_i - \sum_j \Lambda_j^{q,e} q_{ij},$$

then

$$\sum_i \overline{\Lambda}_i^{qT}\Big(\theta_i(q) + H_i^\ell \ell_i(q)\Big) = \Lambda^{qT}\Big(\theta(q) + H^\ell \ell(q)\Big) - \sum_i (\Lambda_1^{q,e}, \ldots, \Lambda_I^{q,e})^T\Big(\theta_i(q) + H_i^\ell \ell_i(q)\Big),$$

so we can then write

$$\mathbb{E}_0\Big[H^q q\Big] = \mathbb{E}_0\Big[R - p - \Lambda^{qT}\Big(\theta(q) + H^\ell \ell(q)\Big)\Big] + \mathbb{E}_0\Big[\sum_i (\Lambda_1^{q,e}, \ldots, \Lambda_I^{q,e})^T\Big(\theta_i(q) + H_i^\ell \ell_i(q)\Big) - (\sum_j \overline{\Lambda}_j^q)^T \Gamma L(q)\Big] - \frac{dC(\Sigma_0^{\hat{L}}, q)}{dq} + \mathbb{E}_0\Big[(\sum_i \overline{\Lambda}_i^q)^T\Big]\Theta_0 \mathbb{E}_0[L(q)].$$

Now, recall that we can write the private FOC, subject to an ex-ante asset tax t_i, as

$$\mathbb{E}_0\Big[H_i^q\Big]q_i = \mathbb{E}_0\Big[R_i - (p_i + t_i) - \Lambda_i^{qT}\Big(\theta_i(q^*) + H_i^\ell \ell_i(q)\Big)\Big] - \mathbb{E}_0\Big[\Lambda_i^{qT}\Big(\tau_i - \Big(\Gamma(\sum_i \overline{\Lambda}_i^\tau) + H_i^\ell \overline{\Lambda}_i^\tau\Big)\tau\Big)\Big].$$

Therefore, stacking and combining the two equations we obtain:

$$\begin{aligned} -t - \mathbb{E}_0\Big[\Psi\tau\Big] = \mathbb{E}_0\Big[\sum_i (\Lambda_1^{q,e}, \ldots, \Lambda_I^{q,e})^T\Big(\theta_i(q) + H_i^\ell \ell_i(q)\Big) \\ - (\sum_j \overline{\Lambda}_j^q)^T \Gamma L(q)\Big] - \frac{dC(\Sigma_0^{\hat{L}}, q)}{dq} + \mathbb{E}_0\Big[(\sum_i \overline{\Lambda}_i^q)^T\Big]\Theta_0 \mathbb{E}_0[L(q)], \end{aligned}$$

where $\mathbb{E}_0\Big[\Psi\tau\Big]$ is the stacking of $\mathbb{E}_0\Big[\Lambda_i^{qT}\Big(\tau_i - \Big(\Gamma(\sum_i \overline{\Lambda}_i^\tau) + H_i^\ell \overline{\Lambda}_i^\tau\Big)\tau\Big)\Big]$. Thus defining $\Lambda^{q,e} = (\Lambda_1^{q,e}, \ldots, \Lambda_I^{q,e})$, we have

$$t = \mathbb{E}_0\Big[(\sum_j \overline{\Lambda}_j^q)^T \Gamma L(q) - \Lambda^{q,eT} \sum_i \Big(\theta_i(q) + H_i^\ell \ell_i(q)\Big)\Big].$$